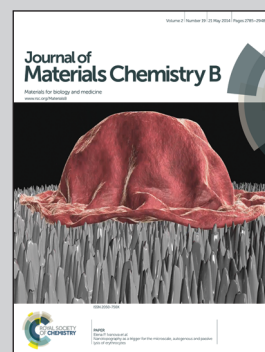


Highlighting research from Prof. Jianzhang Zhao's Laboratory of Molecular Photochemistry & Photophysics, State Key Laboratory of Fine Chemicals, Dalian University of Technology, China.

Title: Cyclometalated Ir(III) complexes with styryl-BODIPY ligands showing near IR absorption/emission: preparation, study of photophysical properties and application as photodynamic/luminescence imaging materials

Heteroleptic C<sup>N</sup> cyclometalated iridium(III) complexes incorporating a monostyryl/distyryl BODIPY ligand showing strong near IR absorption were studied as photodynamic/luminescence imaging materials.

As featured in:



See Jianzhang Zhao *et al.*,  
*J. Mater. Chem. B*, 2014, 2, 2838.



[www.rsc.org/MaterialsB](http://www.rsc.org/MaterialsB)

Registered charity number: 207890

# Cyclometalated Ir(III) complexes with styryl-BODIPY ligands showing near IR absorption/emission: preparation, study of photophysical properties and application as photodynamic/luminescence imaging materials†

Cite this: *J. Mater. Chem. B*, 2014, 2, 2838

Poulomi Majumdar,<sup>‡a</sup> Xiaolin Yuan,<sup>‡b</sup> Shengfu Li,<sup>b</sup> Boris Le Guennic,<sup>c</sup> Jie Ma,<sup>a</sup> Caishun Zhang,<sup>a</sup> Denis Jacquemin<sup>de</sup> and Jianzhang Zhao<sup>\*a</sup>

Heteroleptic C<sup>N</sup> cyclometalated iridium(III) complexes incorporating a monostyryl/distyryl BODIPY ligand via acetylide bonds of 2,2'-bipyridine (bpy) with both absorption (ca.  $\epsilon = 8.96 \times 10^4 \text{ M}^{-1} \text{ cm}^{-1}$ ,  $9.89 \times 10^4 \text{ M}^{-1} \text{ cm}^{-1}$ , and  $7.89 \times 10^4 \text{ M}^{-1} \text{ cm}^{-1}$  at 664 nm, 644 nm, and 729 nm for Ir-2, Ir-3 and Ir-4, respectively) and fluorescence emission bands (ca. 624–794 nm for Ir-1, Ir-2, Ir-3 and Ir-4) in the near infra-red region (NIR) and exceptionally long-lived triplet excited states ( $\tau = 156.5 \mu\text{s}$  for Ir-2) have been reported. Ir(ppy)<sub>3</sub> (Ir-0; ppy = 2-phenylpyridine) was used as reference, which gives the typical weak absorption in visible range ( $\epsilon = 1.51 \times 10^4 \text{ M}^{-1} \text{ cm}^{-1}$  at 385 nm). The nanosecond time-resolved transient absorption and DFT calculations proposed that styryl BODIPY-localized long lived <sup>3</sup>IL states were populated for Ir-1, Ir-2, Ir-3 and Ir-4 ( $\tau_T = 106.6 \mu\text{s}$ ,  $156.5 \mu\text{s}$ ,  $92.5 \mu\text{s}$  and  $31.4 \mu\text{s}$ , respectively) upon photoexcitation. The complexes were used as triplet photosensitizers for singlet oxygen (<sup>1</sup>O<sub>2</sub>) mediated photooxidation of 1,5-dihydronaphthalene to produce juglone. The <sup>1</sup>O<sub>2</sub> quantum yields ( $\Phi_\Delta$ ) of Ir-1 (0.53) and Ir-2 (0.81) are ca. 9-fold of Ir-3 (0.06) and 40-fold of Ir-4 (0.02), respectively. Ir-2 has high molar absorption coefficient at 664 nm, moderate fluorescence in the NIR region, and high singlet oxygen quantum yield ( $\Phi_\Delta = 0.81$ ), exhibits predominate photocytotoxicity over dark cytotoxicity in LLC cells (lung cancer cells) upon irradiation, making it potentially suitable for use in *in vivo* photodynamic therapy (PDT). Our results are useful for preparation of transition metal complexes that show strong absorption of visible light in the NIR region with long-lived triplet excited states and for the application of these complexes in photocatalysis and theranostics such as simultaneous photodynamic therapy (PDT) and luminescent bioimaging.

Received 20th February 2014  
Accepted 4th March 2014

DOI: 10.1039/c4tb00284a

www.rsc.org/MaterialsB

## Introduction

In recent years, near-infrared (NIR) fluorescent probes have drawn considerable attention of chemists in view of their

emerging interest for probing biochemical and biological systems since cellular and tissue imaging in the NIR wavelengths has better tissue penetration and less bioautofluorescence.<sup>1,2</sup> On the other hand, cyclometalated Ir(III) complexes are highly appealing because of their wide range of applications in electroluminescence,<sup>3–12</sup> luminescent molecular probes,<sup>13–22</sup> photodynamic therapy (PDT) for bioimaging,<sup>1</sup> photocatalysis,<sup>23</sup> and more recently triplet-triplet annihilation (TTA) upconversion.<sup>24</sup>

In general, cyclometalated Ir(III) complexes, with short absorption wavelength, weak absorption of visible light and short-lived triplet excited states ( $\tau$ , a few microseconds), are not suitable for application in the newly developed areas, such as photocatalysis,<sup>23a,25</sup> luminescent molecular probes,<sup>15b,17,26</sup> photodynamic therapy and TTA upconversion,<sup>24c</sup> for which strong absorption of visible light and long-lived triplet excited states are preferred.<sup>27</sup>

Concerning the theranostics application, one of the major challenges is to develop new complexes that show strong

<sup>a</sup>State Key Laboratory of Fine Chemical, School of Chemical Engineering, Dalian University of Technology, Dalian, 116024, P.R. China. E-mail: zhaojzh@dlut.edu.cn; Web: <http://finechem.dlut.edu.cn/photochem>; Fax: +86 411-8498-6236

<sup>b</sup>Center Laboratory, Affiliated Zhongshan Hospital of Dalian University, Dalian 116001, P.R. China

<sup>c</sup>Institut des Sciences Chimiques de Rennes, CNRS, Université de Rennes 1, 1 Av. du General Leclerc, 35042 Rennes Cedex, France

<sup>d</sup>Laboratoire CEISAM, UMR CNR 6230, Université de Nantes, 2 Rue de la Houssinière, BP 92208, 44322 Nantes Cedex 3, France

<sup>e</sup>Institut Universitaire de France, 103, bd Saint-Michel, F-75005 Paris Cedex 05, France

† Electronic supplementary information (ESI) available: <sup>1</sup>H, <sup>13</sup>C, and HRMS spectra of the compounds, and photophysical data of the ligands and complexes and coordinates of the optimized geometries of the complexes. See DOI: 10.1039/c4tb00284a

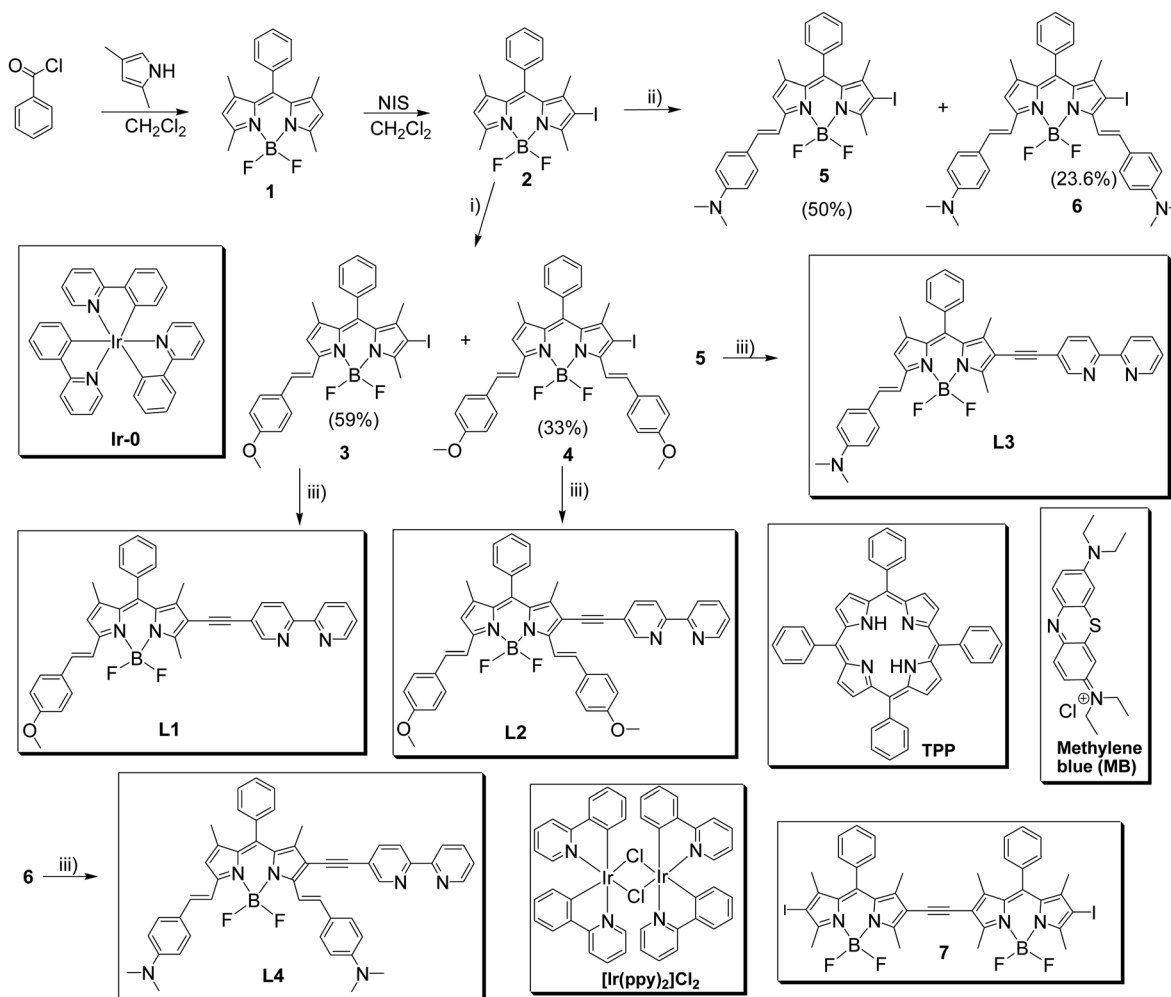
‡ These authors contribute equally to this work.

fluorescence as well as satisfactory intersystem crossing (ISC). These complexes can be used as multi-functional materials, such as photodynamic therapy and at the same time, for luminescent bioimaging. The former application is based on efficient ISC to produce triplet excited states, whereas the latter property is related to efficient radiative decay of singlet excited states. However, for normal transition metal complexes, the ISC is efficient and the luminescence is phosphorescence, thus, the luminescence is substantially dependent on molecular oxygen ( $O_2$ ), which may cause interference for the bioimaging. Fine-tuning the ISC to access balanced strong fluorescence with moderate ISC is difficult and very few transition metal complexes were reported as fluorescence emissive with moderate ISC efficiency.<sup>11b,18</sup>

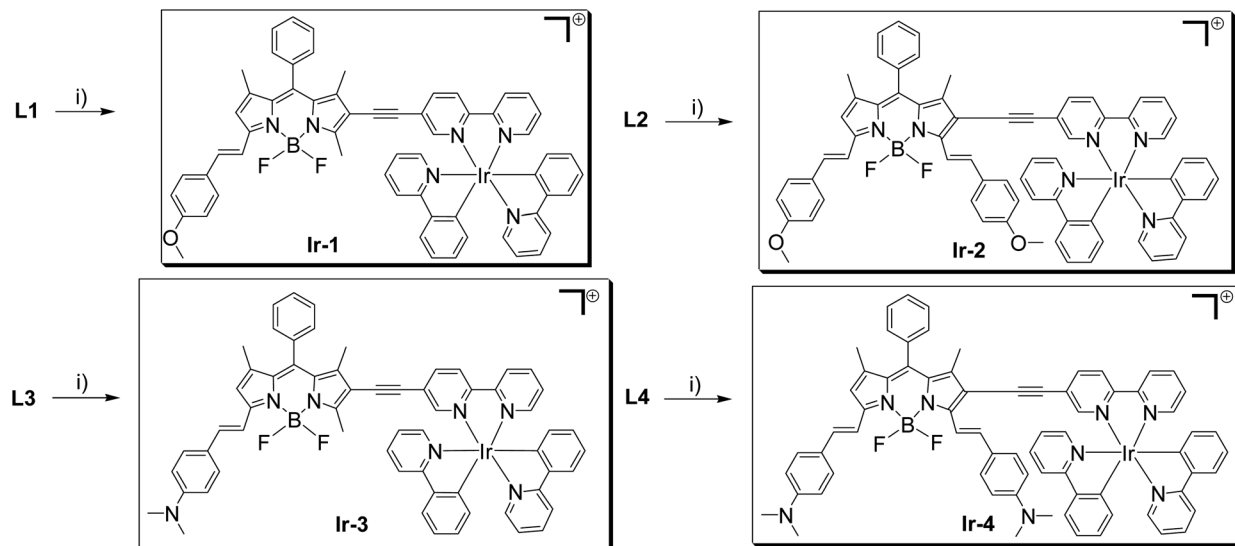
In order to overcome the aforementioned challenge and to develop methods to access transition metal complexes showing strong visible light absorption and long-lived triplet excited states, herein we demonstrate that on attaching bulky organic fluorophores to the coordination center *via* a  $\pi$ -conjugation linker ( $C\equiv C$  triple bond),<sup>27a,28</sup> the heavy atom effect of Ir(III) can

be maximized and the excitation energy can be efficiently funnelled to the triplet excited states thus enhancing the applicability of Ir(III) complexes in photocatalysis or PDT. More importantly, the absorption as well as the emission wavelengths can be extended to the NIR spectral region.

Concerning this aspect, we have prepared four heteroleptic cyclometalated Ir(III) complexes (**Ir-1**, **Ir-2**, **Ir-3** and **Ir-4**, Schemes 1 and 2) using BODIPY ligands to access strong absorption of NIR light through  $\pi$ -conjugation linkers to ensure ISC. Hence, the  $\pi$ -extended styryl derivatives of fluorophore, 4,4'-difluoro-4-bora-3a,4a-diaza-s-indacene (BODIPY), which exhibit remarkable wide-spread applications in biological labelling and cell imaging, as logic gates and ion sensors, and in dye-sensitized solar cells,<sup>29</sup> were used for construction of the ligands. Previously it was found that extension of the ligand  $\pi$ -conjugation induces a strong red shift of the excitation/emission band compared to the unsubstituted complex.<sup>30</sup> Herein, we introduced a bulky methoxyl/methyl diamino mono/di styryl BODIPY ligand *via* acetylide ( $-C\equiv C-$ ) bonds of 2,2'-bipyridine (bpy) to access absorption/fluorescence in the NIR region, with reasonable ISC, as a result



**Scheme 1** Synthesis of the ligands **L1**, **L2**, **L3** and **L4**, the model complex **Ir-0** and *meso*-tetraphenylporphyrin (**TPP**), methylene blue (**MB**) as standard triplet photosensitizers and compound **7** used as the standard for the fluorescence quantum yields are also presented. Reagents and conditions: (i) *p*-methoxybenzaldehyde (4 eq.), toluene, piperidine, AcOH, 120 °C, reflux.; (ii) *p*-(*N,N*-dimethylamino)benzaldehyde (4 eq.), toluene, piperidine, AcOH, 120 °C, reflux.; (iii) 5-ethynyl-2,2'-bipyridine, TEA, THF, Pd(PPh<sub>3</sub>)<sub>4</sub>, CuI, Ar, 85 °C, reflux., 12 h.



Scheme 2 Synthesis of the complexes Ir-1, Ir-2, Ir-3 and Ir-4. The complexes are cationic, and the counter anion  $[\text{PF}_6]^-$  has been omitted for clarity. (i)  $[\text{Ir}(\text{ppy})_2]\text{Cl}_2$ ,  $\text{CH}_2\text{Cl}_2$ -MeOH (2 : 1, v/v), argon, 45 °C, reflux., 6 h.

the complexes show reasonably high fluorescence quantum yields and satisfactory ISC. Thus, the complexes can be used as theranostic reagents for simultaneous luminescent imaging and the photodynamic therapy effect. These properties are exclusive for the normal transition metal complexes.

To date only a few styryl aryl cyclometalated Ir(III) complexes have been reported, application of the triplet excited states and photocatalysis have not been studied,<sup>30,31</sup> although, a BODIPY-containing a tridentate N<sup>^</sup>N<sup>^</sup>N Pt(II) styryl terpyridine complex was reported but with a short luminescence lifetime of 3–4 ns and low fluorescence quantum yield.<sup>32</sup>

Herein, for the first time we have reported the Ir(III) complexes (**Ir-2**, **Ir-3** and **Ir-4**) exhibiting both excitation and emission bands in the NIR region. The photophysical properties have been studied with a steady state and time-resolved spectroscopy, and DFT calculations. Strong absorption in the NIR region (*ca.*  $\epsilon$  is up to  $7.89 \times 10^4 \text{ M}^{-1} \text{ cm}^{-1}$  at 729 nm) and a long-lived triplet excited state ( $\tau = 156.5 \mu\text{s}$ ) were observed, which are unprecedented for Ir(III) complexes. Furthermore, the complexes show strong fluorescence ( $\Phi_{\text{F}}$  is up to 39.9%), as well as moderate ISC property (singlet oxygen quantum yield is up to  $\Phi_{\Delta} = 81\%$ ). We also find that these properties are variable for the complexes. The Ir(III) complexes were used as triplet photosensitizers for singlet oxygen ( $^1\text{O}_2$ ) mediated photooxidation and to investigate the PDT effect in LLC cells (lung cancer cells). These results are useful for designing Ir(III) complexes that show strong absorption of visible light in the NIR region and long-lived triplet excited states, and for the application of these complexes in photocatalysis, theranostics such as PDT/fluorescence bioimaging and non-linear optics.

## Experimental section

### Materials and reagents

All the chemicals are analytically pure and were used as received. Solvents were dried and distilled prior to synthesis.

$\text{IrCl}_3 \cdot 3\text{H}_2\text{O}$  was purchased from Xian Catalyst Chemical Co., Ltd (P. R. China). 5-Ethynyl-2,2'-bipyridine,<sup>33</sup> cyclometalated Ir(III) chloro-bridge dimers  $[\text{Ir}(\text{ppy})_2]\text{Cl}_2$ ,<sup>34</sup> and complex **Ir-0**,<sup>35</sup> were synthesized according to literature methods. For the preparation of compounds **5** and **6**, **L1**, **L2**, **L3** and **L4**, please refer to ESI materials.†

### Synthesis of 3 and 4

**Method A.** To a solution of **2** (250 mg, 0.555 mmol) and *p*-methoxybenzaldehyde (0.27 mL, 2.22 mmol) in dry toluene, acetic acid (1.5 mL) and piperidine (1.5 mL) were added under a  $\text{N}_2$  atmosphere. The reaction mixture was heated at 120 °C under reflux with a Dean Stark trap to remove the water generated by the condensation. The reaction was monitored by TLC ( $\text{CH}_2\text{Cl}_2$ -petroleum ether = 1 : 2 as eluent). After consumption of all the starting materials, the reaction mixture was cooled to room temperature (rt) and the majority of the solvent was evaporated under reduced pressure. Water (150 mL) was added to the residue and the product was extracted from  $\text{CH}_2\text{Cl}_2$  ( $3 \times 100 \text{ mL}$ ). The organic phase was dried over  $\text{Na}_2\text{SO}_4$ , the solvent was evaporated under reduced pressure, and the crude products thus obtained were purified by column chromatography (silica gel,  $\text{CH}_2\text{Cl}_2$ -petroleum ether = 1 : 2, v/v). The first band was collected to obtain a carmine solid as compound **3**. Yield: 186 mg, 59%. mp 223–225 °C.  $^1\text{H NMR}$  (400 MHz,  $\text{CDCl}_3$ ):  $\delta$  7.57–7.50 (m, 6H), 7.30–7.28 (m, 3H), 6.92 (d, 2H,  $J = 12 \text{ Hz}$ ), 6.64 (s, 1H), 3.85 (s, 3H), 2.67 (s, 3H), 1.43 (s, 3H), 1.39 (s, 3H).  $^{13}\text{C NMR}$  (100 MHz,  $\text{CDCl}_3$ ):  $\delta$  161.03, 155.08, 153.24, 144.80, 142.24, 139.85, 137.90, 134.88, 133.32, 129.25, 129.19, 129.16, 128.95, 128.22, 118.34, 116.28, 114.37, 83.72, 55.38, 29.67, 16.36, 14.59. TOF MALDI-HRMS: calcd  $[(\text{C}_{27}\text{H}_{24}\text{BF}_2\text{IN}_2\text{O})^+]$ ,  $m/z = 568.0994$ , found,  $m/z = 568.0970$ . The second band, from the silica gel column chromatography of the same reaction mixture was isolated as a bluish green solid as compound **4**. Yield: 126 mg, 33%. mp 209–211 °C.  $^1\text{H NMR}$

(400 MHz, CDCl<sub>3</sub>):  $\delta$  8.06 (d, 1H,  $J$  = 16 Hz), 7.64–7.58 (m, 6H), 7.52–7.50 (m, 3H), 7.32–7.30 (m, 3H), 6.95 (t, 4H,  $J$  = 8 Hz), 6.67 (s, 1H), 3.87–3.86 (m, 6H), 1.44–1.43 (m, 6H). <sup>13</sup>C NMR (100 MHz, CDCl<sub>3</sub>):  $\delta$  160.88, 160.37, 155.34, 148.14, 144.07, 142.99, 138.12, 137.14, 135.27, 134.00, 132.15, 129.99, 129.46, 129.22, 129.19, 128.95, 128.50, 118.89, 117.20, 116.84, 114.38, 114.26, 81.01, 55.41, 53.45, 17.04, 14.86. TOF MALDI-HRMS: calcd ([C<sub>35</sub>H<sub>30</sub>BF<sub>2</sub>IN<sub>2</sub>O<sub>2</sub>]<sup>+</sup>),  $m/z$  = 686.1413, found,  $m/z$  = 686.1682.

**Method B.** To a solution of **2** (250 mg, 0.555 mmol) and *p*-methoxybenzaldehyde (0.27 mL, 2.22 mmol) in dry toluene, acetic acid (1.5 mL) and piperidine (1.5 mL) were added under a N<sub>2</sub> atmosphere. The reaction mixture was heated at 120 °C under reflux by using a Dean Stark trap and the reaction was monitored by TLC (CH<sub>2</sub>Cl<sub>2</sub>–petroleum ether = 1 : 2 as eluent). The major compound **4** was found to be formed on the TLC plate, the reaction mixture was cooled to rt and the majority of the solvent was evaporated under reduced pressure. Water (150 mL) was added to the residue and the product was extracted from CH<sub>2</sub>Cl<sub>2</sub> (3 × 100 mL). The organic phase was dried over Na<sub>2</sub>SO<sub>4</sub>, evaporated under reduced pressure, and the crude product thus obtained was purified by column chromatography (silica gel, CH<sub>2</sub>Cl<sub>2</sub>–petroleum ether = 1 : 2, v/v). The carmine solid was obtained as compound **3**. Yield: 227 mg, 72%.

Following the similar synthesis procedure, the above reaction mixture was refluxed for 12 h until most of compound **3** was converted to compound **4**, as visualized from TLC (CH<sub>2</sub>Cl<sub>2</sub>–petroleum ether = 1 : 2 as eluent). After that the reaction mixture was cooled to room temperature, the solvent was evaporated, water (150 mL) was added and was extracted from CH<sub>2</sub>Cl<sub>2</sub> (3 × 100 mL). The crude product thus obtained on evaporating the organic phase, was purified by silica gel column chromatography (CH<sub>2</sub>Cl<sub>2</sub>–petroleum ether = 1 : 2, v/v as eluent). The bluish green solid was obtained as compound **4**. Yield: 267 mg, 70%. The spectral data of compound **3/4** obtained by Method B is superimposable with those of Method A.

### Synthesis of L1

To a deaerated solution of compound **3** (114 mg, 0.20 mmol) and 5-ethynyl-2,2'-bipyridine (36 mg, 0.20 mmol) in the mixed solvent of triethylamine (5 mL) and THF (10 mL), Pd(PPh<sub>3</sub>)<sub>4</sub> (11.6 mg, 0.01 mmol, 5 mol%) and CuI (3.8 mg, 0.02 mmol, 10 mol%) were added under an Ar atmosphere. The reaction mixture was refluxed for 12 h at 85 °C. Then the reaction mixture was cooled to rt and the solvent was removed under reduced pressure. The crude product thus obtained, was purified by column chromatography (silica gel, CH<sub>2</sub>Cl<sub>2</sub>–MeOH = 100 : 1, v/v) to give a carmine solid **L1**. Yield: 59.6 mg, 48%. mp 306–308 °C. <sup>1</sup>H NMR (400 MHz, CD<sub>2</sub>Cl<sub>2</sub>):  $\delta$  8.71 (s, 1H), 8.65 (d, 1H,  $J$  = 4 Hz), 8.41–8.38 (m, 2H), 7.84 (dd, 2H,  $J$  = 20 Hz, 8 Hz), 7.58–7.49 (m, 6H), 7.35–7.29 (m, 4H), 6.93 (d, 2H,  $J$  = 8 Hz), 6.68 (s, 1H), 3.83 (s, 3H), 2.71 (s, 3H), 1.54 (s, 3H), 1.46 (s, 3H). <sup>13</sup>C NMR (100 MHz, CD<sub>2</sub>Cl<sub>2</sub>):  $\delta$  161.09, 155.56, 155.14, 151.10, 149.18, 144.79, 141.58, 140.49, 138.73, 138.18, 136.96, 134.65, 134.18, 130.39, 129.25, 129.18, 128.92, 128.22, 123.90, 121.02, 120.12, 118.47, 116.25, 114.40, 114.00, 92.78, 86.70, 70.43, 55.39, 29.67, 14.59, 12.87. TOF MALDI-HRMS: calcd

([C<sub>39</sub>H<sub>31</sub>BF<sub>2</sub>N<sub>4</sub>O + H]<sup>+</sup>),  $m/z$  = 621.2637, found,  $m/z$  = 621.2622; calcd ([C<sub>39</sub>H<sub>31</sub>BF<sub>2</sub>N<sub>4</sub>O]<sup>+</sup>),  $m/z$  = 620.2559, found,  $m/z$  = 620.2589.

### Synthesis of Ir-1

A solution of **L1** (55.8 mg, 0.09 mmol) and [Ir(ppy)<sub>2</sub>]Cl<sub>2</sub> (40.7 mg, 0.038 mmol) in CH<sub>2</sub>Cl<sub>2</sub>–MeOH (15 mL, 1 : 2, v/v) was refluxed for 6 h at 45 °C under an Ar atmosphere. Then the reaction mixture was cooled to rt and a 10-fold excess of NH<sub>4</sub>[PF<sub>6</sub>] was added. The suspension was stirred for 15 min and then filtered to remove the insoluble inorganic salts. The solution was evaporated to dryness under reduced pressure. The crude product was purified by column chromatography (silica gel, CH<sub>2</sub>Cl<sub>2</sub>–MeOH = 20 : 1, v/v) to give a carmine solid **Ir-1** (the solid was washed with hexane to remove the grease). Yield: 72.0 mg, 71.4%. mp 234–236 °C. <sup>1</sup>H NMR (400 MHz, CD<sub>2</sub>Cl<sub>2</sub>):  $\delta$  8.36 (dd, 2H,  $J$  = 8 Hz, 4 Hz), 8.02 (t, 1H,  $J$  = 8 Hz), 7.96–7.92 (m, 2H), 7.87 (d, 2H,  $J$  = 8 Hz), 7.83 (s, 1H), 7.70 (t, 2H,  $J$  = 8 Hz), 7.64 (dd, 2H,  $J$  = 12 Hz, 8 Hz), 7.50–7.40 (m, 8H), 7.36–7.30 (m, 2H), 7.26–7.22 (m, 2H), 6.99 (t, 1H,  $J$  = 8 Hz), 6.94–6.91 (m, 3H), 6.88–6.81 (m, 4H), 6.64 (s, 1H), 6.24 (dd, 2H,  $J$  = 8 Hz, 4 Hz), 3.76 (s, 3H), 2.46 (s, 3H), 1.39 (s, 3H), 1.30 (s, 3H). <sup>13</sup>C NMR (100 MHz, CD<sub>2</sub>Cl<sub>2</sub>):  $\delta$  168.01, 165.99, 165.20, 161.66, 159.89, 157.10, 155.60, 155.54, 155.08, 153.54, 152.64, 150.95, 150.06, 148.91, 146.05, 144.00, 141.53, 140.77, 139.75, 138.60, 135.07, 134.71, 132.35, 132.24, 131.95, 131.06, 130.50, 129.67, 129.05, 128.46, 126.09, 125.27, 125.03, 124.45, 123.73, 123.69, 123.16, 123.08, 120.34, 120.19, 119.48, 116.29, 114.79, 112.46, 92.52, 91.23, 86.29, 55.78, 29.85, 14.79, 12.92. TOF MALDI-HRMS: calcd ([C<sub>61</sub>H<sub>47</sub>BF<sub>2</sub>IrN<sub>6</sub>O]<sup>+</sup>),  $m/z$  = 1121.3502, found,  $m/z$  = 1121.3568. Anal. calcd for [C<sub>61</sub>H<sub>47</sub>BF<sub>2</sub>IrN<sub>6</sub>OP + 2CH<sub>3</sub>OH + C<sub>6</sub>H<sub>14</sub>]: C, 58.51; H, 4.91; N, 5.93. Found: C, 58.35; H, 4.82; N, 5.61.

### Synthesis of L2

To a deaerated solution of **4** (137 mg, 0.20 mmol) and 5-ethynyl-2,2'-bipyridine (36 mg, 0.20 mmol) in the mixed solvent of triethylamine (5 mL) and THF (10 mL), Pd(PPh<sub>3</sub>)<sub>4</sub> (11.6 mg, 0.01 mmol, 5 mol%) and CuI (3.8 mg, 0.02 mmol, 10 mol%) were added under an Ar atmosphere. The reaction mixture was refluxed for 12 h at 85 °C. Thereafter the synthetic procedure is similar to that of **L1**; a bluish green solid **L2** was obtained. Yield: 74.2 mg, 50.2%. mp 298–300 °C. <sup>1</sup>H NMR (400 MHz, CD<sub>2</sub>Cl<sub>2</sub>):  $\delta$  8.31 (d, 1H,  $J$  = 20 Hz), 7.91 (d, 1H,  $J$  = 8 Hz), 7.85 (t, 1H,  $J$  = 8 Hz), 7.69–7.60 (m, 6H), 7.57–7.52 (m, 5H), 7.48–7.44 (m, 1H), 7.37–7.31 (m, 4H), 6.98–6.94 (m, 5H), 6.71 (s, 1H), 3.85–3.86 (m, 6H), 1.58 (s, 3H), 1.47 (s, 3H). <sup>13</sup>C NMR (100 MHz, CD<sub>2</sub>Cl<sub>2</sub>):  $\delta$  161.47, 161.09, 155.68, 150.75, 150.57, 144.71, 143.65, 138.59, 137.41, 135.14, 135.05, 132.33, 132.24, 131.81, 130.09, 129.72, 129.59, 129.41, 129.31, 128.83, 124.29, 124.40, 121.06, 119.08, 117.01, 116.79, 114.78, 111.72, 107.67, 106.87, 70.85, 55.77, 14.99, 13.09. TOF MALDI-HRMS: calcd ([C<sub>47</sub>H<sub>37</sub>BF<sub>2</sub>N<sub>4</sub>O<sub>2</sub> + H]<sup>+</sup>),  $m/z$  = 739.3056, found,  $m/z$  = 739.3011; calcd ([C<sub>47</sub>H<sub>37</sub>BF<sub>2</sub>N<sub>4</sub>O<sub>2</sub>]<sup>+</sup>),  $m/z$  = 738.2978, found,  $m/z$  = 738.2966.

### Synthesis of Ir-2

A solution of **L2** (66.5 mg, 0.09 mmol) and  $[\text{Ir}(\text{ppy})_2]\text{Cl}_2$  (40.7 mg, 0.038 mmol) in  $\text{CH}_2\text{Cl}_2$ -MeOH (15 mL, 1 : 2, v/v) was refluxed for 6 h at 45 °C under an Ar atmosphere. Thereafter the synthetic procedure is similar to that of **Ir-1**. **Ir-2** was obtained as a purple solid (the solid was washed with hexane to remove the grease). Yield: 80.8 mg, 72.5%. mp 296–298 °C.  $^1\text{H}$  NMR (400 MHz,  $\text{CD}_2\text{Cl}_2$ ):  $\delta$  8.50 (d, 2H,  $J = 8$  Hz), 8.09 (dd, 2H,  $J = 16$  Hz, 8 Hz), 7.99–7.89 (m, 5H), 7.81–7.72 (m, 3H), 7.61–7.53 (m, 9H), 7.51–7.47 (m, 3H), 7.44–7.38 (m, 2H), 7.34–7.31 (m, 2H), 7.08–6.84 (m, 10H), 6.74 (s, 1H), 6.29–6.23 (m, 2H), 3.85–3.84 (m, 6H), 1.48 (s, 3H), 1.35 (s, 3H).  $^{13}\text{C}$  NMR (100 MHz,  $\text{CD}_2\text{Cl}_2$ ):  $\delta$  167.74, 167.71, 161.36, 160.83, 156.53, 155.21, 153.53, 152.06, 150.71, 149.57, 149.52, 148.57, 148.52, 145.24, 143.58, 143.53, 143.33, 139.72, 139.47, 139.36, 138.86, 138.26, 138.21, 136.77, 135.15, 134.57, 131.58, 131.50, 131.23, 130.87, 130.74, 129.71, 129.53, 129.47, 129.30, 128.84, 128.41, 128.16, 125.67, 124.92, 124.89, 124.31, 123.37, 123.33, 122.77, 119.96, 119.89, 119.30, 116.46, 116.15, 114.40, 93.69, 92.33, 68.00, 55.43, 14.70, 12.52. TOF MALDI-HRMS: calcd ( $[\text{C}_{69}\text{H}_{53}\text{BF}_2\text{IrN}_6\text{O}_2]^+$ ),  $m/z = 1239.3920$ , found,  $m/z = 1239.3990$ . Anal. calcd for  $[\text{C}_{69}\text{H}_{53}\text{BF}_8\text{IrN}_6\text{O}_2\text{P} + 2\text{CH}_3\text{OH} + \text{C}_6\text{H}_{14}]$ : C, 60.27; H, 4.93; N, 5.48. Found: C, 60.45; H, 4.95; N, 5.24.

### Synthesis of Ir-3

A solution of **L3** (57 mg, 0.09 mmol) and  $[\text{Ir}(\text{ppy})_2]\text{Cl}_2$  (40.7 mg, 0.038 mmol) in  $\text{CH}_2\text{Cl}_2$ -MeOH (15 mL, 1 : 2, v/v) was refluxed for 6 h at 45 °C under an Ar atmosphere. Thereafter the synthetic procedure is similar to that of **Ir-1**; **Ir-3** was obtained as a purple solid (the solid was washed with hexane to remove the grease). Yield: 74.7 mg, 73.2%. mp 254–256 °C.  $^1\text{H}$  NMR (400 MHz,  $\text{CD}_2\text{Cl}_2$ ):  $\delta$  8.42 (dd, 2H,  $J = 16$  Hz, 8 Hz), 8.10 (t, 1H,  $J = 8$  Hz), 8.02–8.00 (m, 2H), 7.95 (d, 2H,  $J = 8$  Hz), 7.91 (s, 1H), 7.80–7.76 (m, 2H), 7.72 (dd, 2H,  $J = 12$  Hz, 8 Hz), 7.56–7.51 (m, 7H), 7.44–7.38 (m, 3H), 7.31 (t, 2H,  $J = 4$  Hz), 7.07 (t, 1H,  $J = 8$  Hz), 7.04–6.99 (m, 3H), 6.96–6.90 (m, 2H), 6.73–6.71 (m, 3H), 6.33–6.30 (m, 2H), 3.05 (s, 6H), 2.53 (s, 3H), 1.46 (s, 3H), 1.36 (s, 3H).  $^{13}\text{C}$  NMR (100 MHz,  $\text{CD}_2\text{Cl}_2$ ):  $\delta$  168.02, 158.50, 155.63, 153.42, 153.21, 152.65, 152.20, 151.83, 151.06, 149.99, 148.95, 148.88, 146.03, 143.98, 141.74, 141.41, 139.71, 139.59, 139.44, 138.73, 138.58, 138.33, 135.46, 134.97, 131.96, 131.84, 131.05, 130.18, 130.12, 129.55, 128.72, 128.38, 126.34, 125.26, 124.89, 124.35, 124.00, 123.67, 123.19, 123.08, 122.94, 121.72, 120.36, 120.18, 119.75, 113.13, 112.28, 111.60, 93.30, 90.98, 40.31, 30.03, 15.11, 12.83. TOF MALDI-HRMS: calcd ( $[\text{C}_{62}\text{H}_{50}\text{BF}_2\text{IrN}_7]^+$ ),  $m/z = 1134.3818$ , found,  $m/z = 1134.3732$ . Anal. calcd for  $[\text{C}_{62}\text{H}_{50}\text{BF}_8\text{IrN}_7\text{P} + 2\text{CH}_3\text{OH}]$ : C, 57.23; H, 4.35; N, 7.30. Found: C, 57.39; H, 4.59; N, 6.99.

### Synthesis of Ir-4

A solution of **L4** (68.8 mg, 0.09 mmol) and  $[\text{Ir}(\text{ppy})_2]\text{Cl}_2$  (40.7 mg, 0.038 mmol) in  $\text{CH}_2\text{Cl}_2$ -MeOH (15 mL, 1 : 2, v/v) was refluxed for 6 h at 45 °C under an argon atmosphere. Thereafter the synthetic procedure is similar to that of **Ir-1**; a greyish green solid compound **Ir-4** was obtained (the solid was washed with

hexane to remove the grease). Yield: 74.7 mg, 65.6%.  $^1\text{H}$  NMR (400 MHz,  $\text{CD}_2\text{Cl}_2$ ):  $\delta$  8.71 (dd, 2H,  $J = 12$  Hz, 8 Hz), 8.14 (t, 1H,  $J = 8$  Hz), 8.08 (d, 1H,  $J = 8$  Hz), 7.98–7.89 (m, 5H), 7.85–7.80 (m, 1H), 7.75 (dd, 3H,  $J = 16$  Hz, 8 Hz), 7.60 (t, 2H,  $J = 8$  Hz), 7.55–7.52 (m, 5H), 7.48–7.39 (m, 6H), 7.36–7.32 (m, 3H), 7.05 (dd, 2H,  $J = 16$  Hz, 8 Hz), 7.00–6.97 (m, 1H), 6.92 (t, 1H,  $J = 8$  Hz), 6.88–6.84 (m, 1H), 6.74–6.70 (m, 5H), 6.27 (dd, 2H,  $J = 16$  Hz, 8 Hz), 3.04–3.03 (m, 12H), 1.46 (s, 3H), 1.32 (s, 3H).  $^{13}\text{C}$  NMR (100 MHz,  $\text{CD}_2\text{Cl}_2$ ):  $\delta$  167.78, 162.03, 156.76, 155.37, 153.37, 152.00, 151.76, 151.28, 151.12, 150.59, 149.73, 149.58, 148.58, 148.49, 144.37, 143.60, 143.51, 142.12, 140.37, 139.57, 138.20, 138.12, 137.29, 136.57, 134.98, 131.60, 131.53, 131.01, 130.75, 129.71, 129.12, 128.80, 128.75, 128.02, 127.76, 125.88, 125.79, 125.30, 124.90, 124.76, 124.68, 124.01, 123.31, 122.77, 122.71, 119.96, 119.84, 119.17, 113.92, 113.31, 112.08, 111.95, 94.55, 92.15, 70.49, 40.03, 39.93, 29.66, 14.65, 12.41. TOF MALDI-HRMS: calcd ( $[\text{C}_{71}\text{H}_{59}\text{BF}_2\text{IrN}_8]^+$ ),  $m/z = 1265.4553$ , found,  $m/z = 1265.4539$ . Anal. calcd for  $[\text{C}_{71}\text{H}_{59}\text{BF}_8\text{IrN}_8\text{P} + 2\text{CH}_3\text{OH} + \text{C}_6\text{H}_{14}]$ : C, 60.80; H, 5.23; N, 7.18. Found: C, 60.61; H, 5.02; N, 7.08.

### Analytical measurements

$^1\text{H}$  and  $^{13}\text{C}$  NMR spectra were recorded on a Bruker 400 and 100 MHz spectrophotometer, respectively ( $\text{CDCl}_3$  or  $\text{CD}_2\text{Cl}_2$  as solvent, TMS as standard,  $\delta = 0.00$  ppm). High resolution mass spectra (HRMS) were determined on a MALDI TOF micro MX spectrometer. Elemental analysis was carried out with a VarioEL III Element analyzer (Elementar, Germany) and was in agreement with the calculated values within  $\pm 0.4\%$ . Fluorescence spectra were measured on a RF-5301PC spectrofluorometer (Shimadzu). Fluorescence quantum yields were measured with compound **7** as standard ( $\Phi_{\text{F}} = 9.3\%$  in toluene).<sup>36</sup> Phosphorescence quantum yields were measured with  $\text{Ru}(\text{dmb})_3[\text{PF}_6]_2$  as standard ( $\Phi_{\text{P}} = 7.3\%$  in deaerated  $\text{CH}_3\text{CN}$ ,  $\text{dmb} = 4,4'$ -dimethyl-2,2'-bipyridine). Fluorescence lifetimes were measured with an OB920 luminescence lifetime spectrometer (Edinburgh, UK). Absorption spectra were recorded on an Agilent 8453A UV/Vis spectrophotometer. The nanosecond time-resolved transient difference absorption spectra were recorded on a LP 920 laser flash photolysis spectrometer (Edinburgh Instruments, Livingston, UK). The sample solutions were purged with  $\text{N}_2$  for 15 min before measurement. The samples were excited with a 355 or 532 nm nanosecond pulsed laser, and the transient signals were recorded on a Tektronix TDS 3012B oscilloscope. The lifetime values (by monitoring the decay traces of the transients) were obtained with the LP920 software.

### DFT calculations

The density functional theory (DFT) calculations were used for optimization of both singlet states and triplet states. The UV-Vis absorption and the energy level of the  $\text{T}_1$  state were calculated with the time dependent DFT (TDDFT), based on the optimized singlet ground state geometries ( $\text{S}_0$  state). The spin density surfaces of the complexes were calculated based on the optimized triplet states. All the calculations were performed at the B3LYP/GENECP/LANL2DZ or M062X/GENECP/LANL2DZ level

with Gaussian 09W.<sup>37</sup> Toluene was used as the solvent for the calculations (CPCM model).

### Photooxidation

10 mL CH<sub>2</sub>Cl<sub>2</sub>-MeOH (9/1, v/v) solution containing 1,5-dihydro-naphthalene (DHN,  $2.0 \times 10^{-4}$  M) and a photosensitizer ( $2.0 \times 10^{-5}$  M) was placed in a round-bottom flask and was irradiated by a 35 W xenon lamp through a 0.72 M NaNO<sub>2</sub> solution to cut off the light with a wavelength shorter than 385 nm. At intervals of 2–5 min, 2 mL of the mixture was sampled for the UV/Vis absorption measurement and was put back immediately after recording the absorption spectra, and UV/Vis absorption spectra were recorded using the Agilent 8453 UV/Vis spectrophotometer. The power density was tuned to 20 mW cm<sup>-2</sup> and was measured with a solar power meter. The DHN consumption was monitored by a decrease in the absorption at 301 nm, the concentration of DHN was calculated by using its molar absorption coefficient ( $\epsilon = 7664 \text{ M}^{-1} \text{ cm}^{-1}$ ) at 301 nm. The juglone production was monitored by an increase in the absorption at 427 nm, the concentration of juglone was calculated by using its molar absorption coefficient ( $\epsilon = 3811 \text{ M}^{-1} \text{ cm}^{-1}$ ), and the yield of juglone was obtained by dividing the concentration of juglone with the initial concentration of DHN.

### Singlet oxygen (<sup>1</sup>O<sub>2</sub>) quantum yields ( $\Phi_{\Delta}$ )

$\Phi_{\Delta}$  values of the triplet photosensitizers were measured according to a modified literature method,<sup>38</sup> with MB ( $\Phi_{\Delta} = 0.57$  in dichloromethane) as standard.<sup>39</sup> Quantum yields for singlet oxygen generation in CH<sub>2</sub>Cl<sub>2</sub> were determined by monitoring the photooxidation of 1,3-diphenylisobenzofuran (DPBF) sensitized by the iridium complexes. 1,3-Diphenylisobenzofuran (DPBF) was used as the <sup>1</sup>O<sub>2</sub> scavenger, due to its fast reaction with <sup>1</sup>O<sub>2</sub>. The absorbance of DPBF was adjusted to around 1.0 at 414 nm in air saturated CH<sub>2</sub>Cl<sub>2</sub>. Then, the photosensitizer was added to cuvette and photosensitizer's absorbance was adjusted to around 0.2–0.3. Then, the cuvette was exposed to monochromatic light at the specific wavelength for 10 seconds depending on the efficiency of the triplet photosensitizers. The photosensitizer and MB were irradiated with the same wavelength. Absorbance was measured six times after each irradiation. Then, the slopes of the curves of absorbance maxima of DPBF at 414 nm *versus* irradiation time for each photosensitizer were calculated. Singlet oxygen quantum yields ( $\Phi_{\Delta}$ ) were calculated according to the equation (eqn (1)):

$$\Phi_{\Delta\text{sam}} = \Phi_{\Delta\text{std}} \left( \frac{m_{\text{sam}}}{m_{\text{std}}} \right) \left( \frac{F_{\text{std}}}{F_{\text{sam}}} \right) \quad (1)$$

where “sam” and “std” designate the “Ir(III) photosensitizers” and “MB”, respectively. “*m*” is the slope of difference in change in absorbance of DPBF (at 414 nm) with the irradiation time, “*F*” is the absorption correction factor, which is given by  $F = 1 - 10^{-\text{OD}}$  (OD is the absorbance at the irradiation wavelength).

### Cell culture

LLC cells (lung cancer cells) were maintained at a density of  $1.0 \times 10^6$  cells per mL for confocal imaging in Roswell Park

Memorial Institute (RPMI)-1640 Medium supplemented with Foetal Bovine Serum (FBS) (10%) and penicillin (100 U mL<sup>-1</sup> culture medium), streptomycin (100 μg mL<sup>-1</sup> culture medium), NaHCO<sub>3</sub> (2 g L<sup>-1</sup>), and 1% antibiotics (penicillin–streptomycin, 100 U mL<sup>-1</sup>). Cultures were grown in a humidified incubator at 37 °C, 5% CO<sub>2</sub>, and 95% relative humidity. Similarly, 1121 cells were cultured.

For trypan blue staining, exponentially growing, LLC cells were seeded at a density of  $1.0 \times 10^6$  cells per well, in triplicate, and 24 h later they were treated with different concentrations (1 μM, 10 μM and 20 μM) of Ir(III) complexes in DMSO as individual entities, at 37 °C in a humidified 5% CO<sub>2</sub> atmosphere for the below mentioned time periods. Then, cells were kept either in the dark or were illuminated with a 635 nm LED for a period of 4 h at 37 °C in a humidified incubator containing 5% CO<sub>2</sub>. To evaluate the cell viability of the dye, wells that had been irradiated for 4 h were incubated in the dark for a further 24 h. Untreated LLC cells were used as controls. As controls, plates kept in the dark for 4 h were also incubated for an additional 24 h. After the appropriate incubation period, the medium was removed and the cells were washed with PBS for three times, prior to cell imaging. Confocal fluorescence imaging studies were performed on a Nikon ECLIPSE-Ti confocal laser scanning microscope.

To study the cell death induced by Ir(III) complexes upon PDT treatment on LLC cells, after the appropriate incubation period, the medium of each well was collected, rinsed with PBS for three times, and trypsinized followed by centrifugation. The cells were re-suspended, collected and mixed with the same volume of 0.4% trypan blue solution. Cells were allowed to stand from 5 to 15 min. The viable (unstained) and dead (stained) cells was visualised with a light microscope. All compounds used were prepared as a stock in DMSO, immediately before use.

## Results and discussion

### Design and synthesis of the complexes

Our strategy for the formation of heteroleptic Ir(III) centred complexes containing 2,2'-bipyridine based ligands has been rationalized on the fact to maximize the heavy atom effect exerted by Ir(III) on the styryl BODIPY ligand. A  $\pi$ -conjugation linker was used, a typical strategy to access strong visible light-absorption, long-lived triplet excited states and efficient ISC in transition metal complexes.<sup>40,41</sup> The styryl BODIPY and its respective bulky ligand have been introduced to extend the UV-Vis absorption wavelength and fluorescence emission to the NIR region, respectively.<sup>30</sup> Initially, the Knoevenagel condensation reaction of 2-iodo BODIPY with *p*-methoxybenzaldehyde was carried out, which regioselectively at the 5-position of the BODIPY moiety led to the formation of 5-monostyryl BODIPY derivative **3** as the major product along with 3,5-distyryl BODIPY derivative **4** as the minor product (Scheme 1). The molecular structure of both the derivatives **3** and **4**, thus isolated by column chromatography were confirmed by <sup>1</sup>H NMR and 2D COSY NMR, in particular by the shift in the peak due to the  $\beta$ -pyrrolic proton at the 6-position of the BODIPY from  $\delta$  6.0 to *ca.* 6.6 ppm, due to the formation of the styryl group at the

5-substitution position. The data were consistent with those of previously reported mono<sup>42–45</sup> and distyryl BODIPY dyes.<sup>29c,46</sup> Similarly, 5-monostyryl BODIPY derivative **5** and 3,5-distyryl BODIPY derivative **6** were synthesized and characterized (Scheme 1).

Pd(0)-catalyzed Sonogashira coupling reactions of 2-iodo styryl BODIPY derivatives and 5-ethynyl-2,2'-bipyridine were carried out to form bulky  $\pi$ -extended styryl BODIPY ligands (Scheme 1) to enhance UV-Visible absorption wavelength and fluorescence emission of the Ir(III) centred complexes. Ir(III) complexes were synthesized from the bis(pyridylphenyl)-iridium(III) dichloride intermediate (Scheme 2).<sup>59</sup> **Ir-0** was prepared as the model complex for photophysical studies. All the complexes were obtained with moderate to satisfactory yields.

### UV-Vis absorption spectra of the complexes

The UV-Vis absorption of the styryl BODIPY ligands and Ir(III) complexes were studied (Fig. 1). Styryl BODIPY based ligands **L1**, **L2**, **L3** and **L4** exhibited intense absorption maxima at 605 nm ( $\epsilon = 1.03 \times 10^5 \text{ M}^{-1} \text{ cm}^{-1}$ ), 666 nm ( $\epsilon = 1.13 \times 10^5 \text{ M}^{-1} \text{ cm}^{-1}$ ), 639 nm ( $\epsilon = 1.23 \times 10^5 \text{ M}^{-1} \text{ cm}^{-1}$ ) and 723 nm ( $\epsilon = 6.89 \times 10^4 \text{ M}^{-1} \text{ cm}^{-1}$ ), respectively in UV-Vis absorption (Fig. 1a). UV-Vis absorption spectra of the model complex **Ir-0** showed maxima for the typical cyclometalated Ir(III) complex in the UV range ( $\epsilon = 4.98 \times 10^4 \text{ M}^{-1} \text{ cm}^{-1}$  at 284 nm) and a very weak absorption in the visible-light range ( $\epsilon = 1.51 \times 10^4 \text{ M}^{-1} \text{ cm}^{-1}$  at 385 nm) (Fig. 1b).<sup>15,47</sup>

In contrast, styryl BODIPY based heteroleptic cyclometalated Ir(III) complexes displayed strong absorption maxima at 606 nm ( $\epsilon = 1.14 \times 10^5 \text{ M}^{-1} \text{ cm}^{-1}$ ) for **Ir-1**, and in the NIR region at 664 nm ( $\epsilon = 8.96 \times 10^4 \text{ M}^{-1} \text{ cm}^{-1}$ ), 644 nm ( $\epsilon = 9.89 \times 10^4 \text{ M}^{-1} \text{ cm}^{-1}$ ) and 729 nm ( $\epsilon = 7.89 \times 10^4 \text{ M}^{-1} \text{ cm}^{-1}$ ) for **Ir-2**, **Ir-3** and **Ir-4**, respectively (Fig. 1b). No significant wavelength shift upon complexation with Ir(III) was observed. This demonstrates that the molecular orbitals of the ligands remained unaltered to a large extent on complexation. From the absorption of the ligands and complexes, it was observed that distyryl BODIPY induced *ca.* 58 nm (for methoxy substituent) and *ca.* 85 nm (for dimethyl amino substituent) of red shifts for the respective ligands and complexes as compared to the respective monostyryl BODIPY, owing to a more

intramolecular charge transfer (ICT) effect due to the large extended  $\pi$  conjugation in distyryl in comparison to monostyryl. Approximately, 38 nm and 65 nm of red shifts for the absorption of ligands and complexes were observed in the case of methoxy monostyryl BODIPY compared to amino dimethyl monostyryl BODIPY. Similar changes were observed for methoxy distyryl BODIPY vs. amino dimethyl distyryl BODIPY. This red shift is due to the more significant intramolecular charge transfer (ICT) in styryl BODIPY ligands and complexes with a dimethyl amino group. The characteristic absorption spectrum together with the excitation and emission spectra of complexes **Ir-1**, **Ir-2**, **Ir-3** and **Ir-4** are shown in Fig. 2.

### The luminescence spectra of the compounds

The photoluminescence of the compounds was studied (Fig. 3). The ligands **L1**, **L2**, **L3** and **L4** give strong fluorescence in the NIR region at 625 nm ( $\Phi_F = 68.6\%$ ), 684 nm ( $\Phi_F = 35.6\%$ ), 674 nm ( $\Phi_F = 24.5\%$ ) and 758 nm ( $\Phi_F = 10.3\%$ ), respectively (Fig. 3a and Fig S43<sup>†</sup>). The dual emission was observed for **L2** at 684 nm

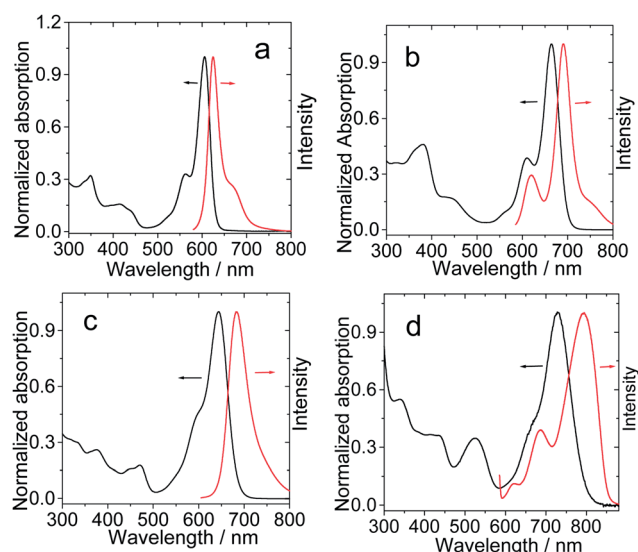


Fig. 2 Normalized absorption spectra (black) and fluorescence spectra (red) ( $c = 1.0 \times 10^{-5} \text{ M}$  in toluene): (a) **Ir-1**, (b) **Ir-2**, (c) **Ir-3** and (d) **Ir-4**.

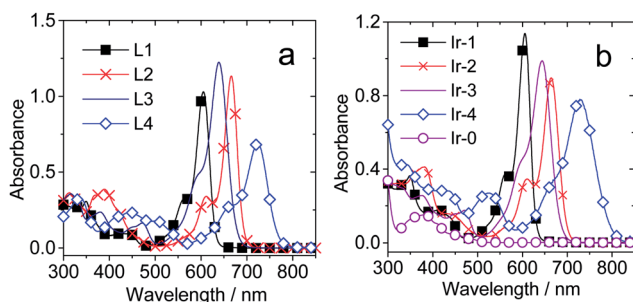


Fig. 1 UV-Vis absorption spectra of the (a) ligands **L1**, **L2**, **L3** and **L4** and (b) complexes **Ir-1**, **Ir-2**, **Ir-3**, **Ir-4** and **Ir-0**.  $c = 1.0 \times 10^{-5} \text{ M}$  in toluene. 20 °C.

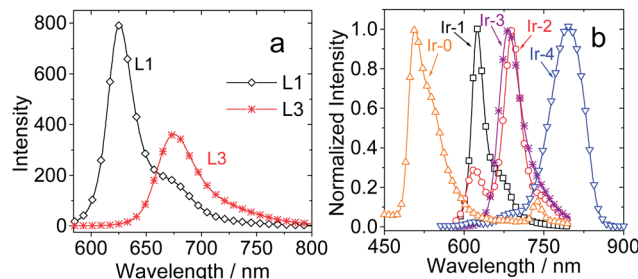


Fig. 3 (a) Fluorescence spectra of ligands **L1** and **L3** and (b) normalized fluorescence spectra of complexes **Ir-1**, **Ir-2**, **Ir-3**, **Ir-4** and **Ir-0**. ( $\lambda_{\text{exc}} = 580 \text{ nm}$ ,  $c = 1.0 \times 10^{-5} \text{ M}$  in toluene). 20 °C.

and 619 nm and for **L4** at 758 nm and 659 nm. A similar trend was observed for the complexes with fluorescence quantum yields ( $\Phi_F$ ) of 39.9%, 13.2%, 32.6% and 1.0% for **Ir-1**, **Ir-2**, **Ir-3** and **Ir-4**, respectively (Fig. 3b and Table 3). The appearance of two emission peaks can be attributed to the  $S_2$  emission of the chromophores, presumably due to a Franck Condon barrier for the internal conversion of  $S_2 \rightarrow S_1$ . Another possible origin for the minor emission shoulder at higher energy side of the emission band is due to the vibrational structure of the luminescence. Both the peaks exhibit similar behaviour on increasing the concentration (see ESI, Fig. S49b and S49d†) and on varying the excitation wavelength (Fig. S50b and S50d†) suggesting that the two emission peaks are from the same species.

Intramolecular charge transfer was proved by the concentration-dependent and excitation-energy dependence behaviour of emission spectra of **Ir-2** and **Ir-4**. Due to the large ICT effect in the distyryl group and styryl BODIPY with an amino substituent, the emission was red shifted for distyryl and dimethyl amino styryl BODIPY ligands and complexes as compared to that of monostyryl and styryl BODIPY with a methoxy group, respectively (Fig. 4 and S43†).

In contrast to ligands, the complexes show weaker fluorescence (Fig. 5). The fluorescence emission of the ligands was remarkably quenched in the complexes which indicated efficient intersystem crossing (ISC) from the singlet excited states to the triplet excited states of the complexes upon visible light photoexcitation.<sup>35</sup> ISC is weaker in **Ir-2**. Such a result is rarely observed for cyclometalated Ir(III) complexes, e.g. in an Ir(III) coordination center with a BODIPY fluorophore, the fluorescence emission of the BODIPY could not be completely quenched rather, the phosphorescence of the Ir(III) coordination center was quenched instead.<sup>48</sup> Thus, the ISC in **Ir-1** to **Ir-4** may have been aroused due to the direct association of the  $\pi$ -core of the styryl BODIPY fluorophore to the Ir(III) coordination centres, which was not the case for some of the previous Ir(III) complexes that contained a bulky organic chromophore.<sup>11b,35,48</sup>

**Ir-1**, **Ir-2**, **Ir-3** and **Ir-4** were not sensitive to  $O_2$ , thus exhibits no phosphorescence (see ESI, Fig. S42†). The model complex **Ir-0** gave a structureless intense emission band at 507 nm and the

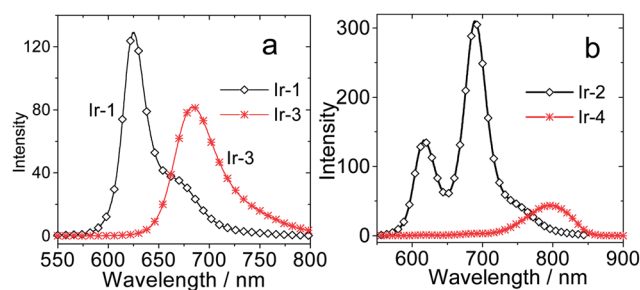


Fig. 4 Comparison of the emission intensities of the complexes: (a) **Ir-1** and **Ir-3**,  $\lambda_{ex} = 496$  nm and (b) **Ir-2** and **Ir-4**,  $\lambda_{ex} = 546$  nm.  $c = 1 \times 10^{-5}$  M in toluene. 20 °C.

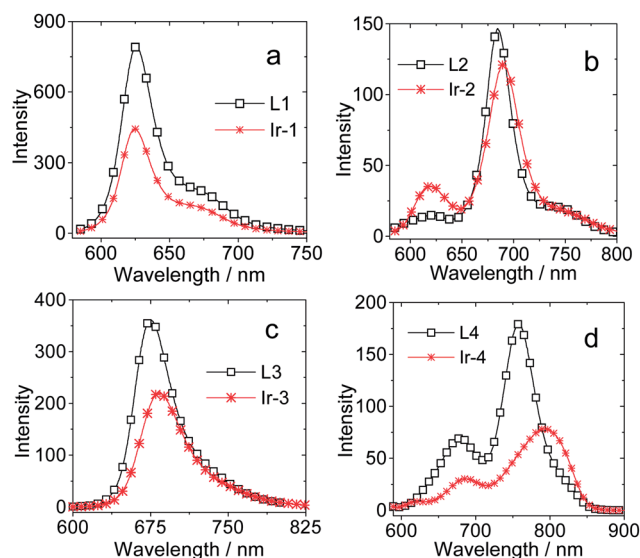


Fig. 5 Comparison of the emission intensities of the ligands and complexes: (a) **L1** and **Ir-1**,  $\lambda_{ex} = 580$  nm; (b) **L2** and **Ir-2**,  $\lambda_{ex} = 580$  nm; (c) **L3** and **Ir-3**,  $\lambda_{ex} = 580$  nm and (d) **L4** and **Ir-4**,  $\lambda_{ex} = 580$  nm.  $c = 1 \times 10^{-5}$  M in toluene. 20 °C.

emission can be significantly quenched by  $O_2$ . The structureless intense emission indicates that the emission is from a  $^3MLCT$  excited state.

**Table 1** Electronic excitation energies (eV) and corresponding oscillator strengths ( $f$ ), main configurations and CI coefficients of the low-lying electronic excited states of complex **Ir-1** calculated by TDDFT//B3LYP/LANL2DZ based on the DFT//B3LYP/LANL2DZ optimized ground state geometries

TDDFT//B3LYP/GENECP						
	Electronic transition	Energy <sup>a</sup> [eV nm <sup>-1</sup> ]	$f^b$	Composition <sup>c</sup>	CI <sup>d</sup>	Character
Singlet	$S_0 \rightarrow S_1$	1.93/643	1.2242	H $\rightarrow$ L	0.7019	ILCT
	$S_0 \rightarrow S_2$	2.28/544	0.8532	H $\rightarrow$ L+1	0.6895	ILCT
	$S_0 \rightarrow S_5$	2.77/448	0.3269	H-2 $\rightarrow$ L	0.5733	MLCT/LLCT
	$S_0 \rightarrow S_7$	2.98/417	0.1228	H-1 $\rightarrow$ L+1	0.4248	MLCT/LLCT
	$S_0 \rightarrow S_{17}$	3.29/376	0.1407	H-4 $\rightarrow$ L+1	0.6329	ILCT
Triplet	$S_0 \rightarrow T_1$	1.23/1012	0.0000 <sup>e</sup>	H $\rightarrow$ L+1 H $\rightarrow$ L	0.5304 0.4475	ILCT ILCT

<sup>a</sup> Only the selected low-lying excited states are presented. <sup>b</sup> Oscillator strengths. <sup>c</sup> Only the main configurations are presented. <sup>d</sup> The CI coefficients are in absolute values. <sup>e</sup> No spin-orbital coupling effect was considered, thus the  $f$  values are zero.

### Solvent-dependency of the UV-Vis absorption and the luminescence spectra of the complexes

The study of the solvent dependency of the complexes was carried out with the intention to study the properties of the emissive excited state of the complexes. The UV-Vis absorption of **Ir-1**, **Ir-2**, **Ir-3**, and **Ir-4** (Fig. 6 & S45<sup>†</sup>) along with the respective ligands (Fig. S44 & S45<sup>†</sup>) does not show significant solvent dependency, indicating that the ground states were not affected by the solvent polarity or hydrogen bonding. We noted that the complexes are soluble in aqueous solution (MeOH–H<sub>2</sub>O, 8 : 2, v/v).

On comparison, the emissions of the complexes are more sensitive to the polarity of the solvents (Fig. 7 and S48<sup>†</sup>). For **Ir-1** and **Ir-2**, the emission intensity is slightly increased in solvents with high polarity and displayed hypsochromic shift with increasing solvent polarity. This distinctive property for **Ir-1** and **Ir-2** may be attributed to the decreased energy gap between ground and excited states with increased possibility of transition on increasing the polarity. In contrast, bathochromic shift was observed in the case of amino dimethyl substituted complexes **Ir-3** and **Ir-4** and the respective emission intensity is completely quenched in high polar solvents, thus suggesting the activation of the non-emissive decay channel in high polar solvents. Energy gap law may also play a role in this change of the fluorescence quantum yield. Based on these results, we propose that the emission of the complexes is influenced by the polarity of the solvents and amino dimethyl styryl BODIPY Ir(III) complexes have more significant ICT than the methoxyl styryl BODIPY in high polar solvents. These results were further

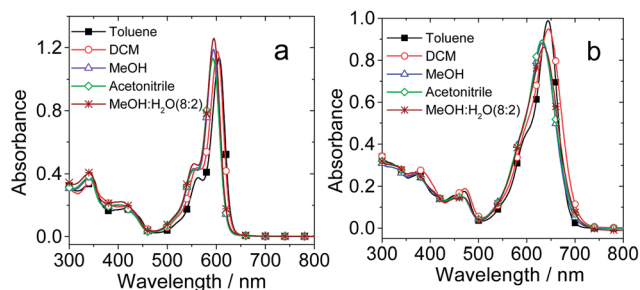


Fig. 6 Solvent-polarity-dependence of the absorption of the complexes (a) **Ir-1** and (b) **Ir-3**.  $c = 1.0 \times 10^{-5}$  M. 20 °C.

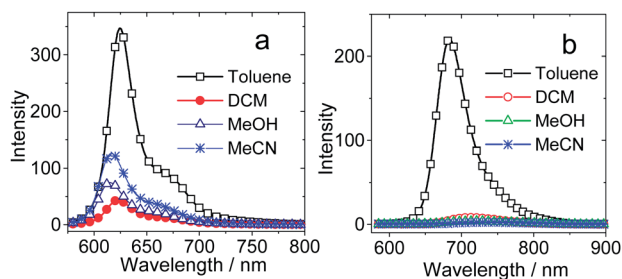


Fig. 7 Solvent-polarity-dependence of the emission of the complexes ( $c = 1.0 \times 10^{-5}$  M): (a) **Ir-1**,  $\lambda_{\text{ex}} = 570$  nm and (b) **Ir-3**,  $\lambda_{\text{ex}} = 595$  nm. 20 °C.

supported by the increased fluorescence quantum yield and life time with increasing solvent polarity for **Ir-1** and **Ir-2** whereas these were decreased in the case of **Ir-3** and **Ir-4**. For **Ir-0** no considerable effect was observed towards solvent polarity.

The absorption and emission spectra of **Ir-1**, **Ir-2**, **Ir-3** and **Ir-4** are shown in (Fig. 2) and Stokes shifts are tabulated in Table 3. Stokes shifts ( $\Delta_{\text{st}}$ ) were found to be higher for **Ir-3** and **Ir-4** compared to **Ir-1** and **Ir-2**, respectively.

### Nanosecond time-resolved transient difference absorption spectroscopy

The nanosecond time-resolved transient difference absorption spectra of the complexes were studied so as to investigate the triplet excited states of the complexes (Fig. 8, see ESI Fig. S51–S53<sup>†</sup>). Upon 532 nm pulsed laser excitation, positive transient absorption (TA) bands at 374 and 665 nm were observed for **Ir-1** (Fig. 8a) along with the bleaching bands at 429 nm and 600 nm due to the UV-Vis absorption (Fig. 1b). Based on these results, we conclude that the triplet excited state of **Ir-1** is localized on the styryl BODIPY ligand, not on the Ir(III) coordination center. The transient signal was quenched in aerated solution, which proves the triplet feature of the transients. The lifetime of the triplet excited state was determined to be 106.6  $\mu\text{s}$ .

Similarly, upon 532 nm photoexcitation, the bleaching band at 662 nm was observed for **Ir-2** (Fig. 8c) which is also consistent with the UV-Vis absorption spectra (Fig. 1b). This implies that the triplet excited state of **Ir-2** is also localized on the styryl BODIPY ligand and not on the Ir(III) coordination center. The lifetime of the triplet excited state was determined to be 156.5  $\mu\text{s}$  for **Ir-2** which was also found to be quenched in aerated solution. The transient absorption spectrum of **Ir-3** (see ESI, Fig. S51<sup>†</sup>) was found to be similar to that of **Ir-1**, with a slightly blue-shifted bleaching band at 632 nm and positive transient absorption bands at about 408 nm and 760 nm. The lifetime of

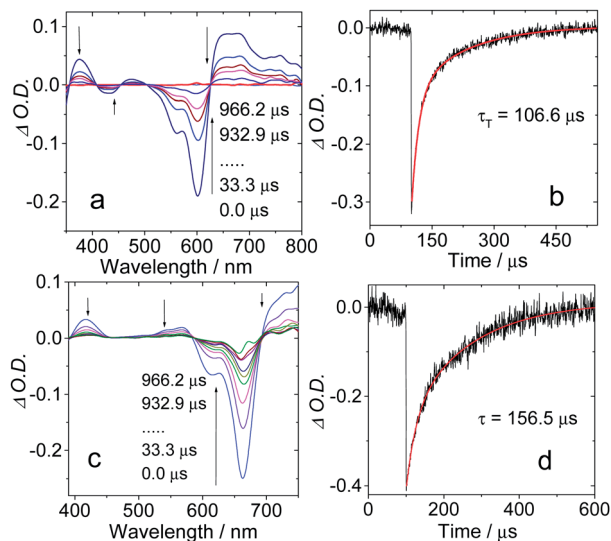


Fig. 8 Nanosecond time-resolved transient difference absorption spectra after pulsed excitation: (a) **Ir-1** and (c) **Ir-2** and decay traces of (b) **Ir-1** and (d) **Ir-2**.  $\lambda_{\text{ex}} = 532$  nm,  $c = 1.0 \times 10^{-5}$  M in toluene. 20 °C.

the transient was determined to be 92.5  $\mu\text{s}$ . To the best of our knowledge, these values are the longest triplet state lifetimes observed for the styryl BODIPY group in transition metal complexes.<sup>32</sup> The lifetime of the triplet excited state for **Ir-4** was found to be 31.4  $\mu\text{s}$ . These <sup>3</sup>IL state lifetime values are close to those of Styryl BODIPY-C<sub>60</sub> Dyads (105.6  $\mu\text{s}$ /123.2  $\mu\text{s}$ )<sup>49</sup> but much longer than that observed for the iodo-styryl BODIPY (4  $\mu\text{s}$ ).<sup>36</sup> Previously the triplet excited state lifetimes of the BODIPY-containing Ir(III) complexes were reported as 87.2  $\mu\text{s}$ .<sup>28b</sup>

In disagreement to **Ir-1**, **Ir-2**, **Ir-3** and **Ir-4**, a notably different transient profile was observed for **Ir-0** with a transient absorption band at 320 nm along with a bleaching band at 525 nm due to the strong phosphorescence emission (see ESI Fig. S51d†). The lifetime of the triplet excited state for **Ir-0** was found to be 1.34  $\mu\text{s}$ . Thus, **Ir-0** was distinguished in the <sup>3</sup>MLCT state.

### DFT calculations: assignment of the excited states

From a theoretical perspective, the photophysical properties of transition metal complexes were studied by density functional theory (DFT) calculations.<sup>27a,41i,50</sup> In order to study the lowest-lying triplet excited states of the complexes, the localization of spin density surfaces of the complexes were studied.<sup>24d,27a,28a,41i,51</sup> The spin density surfaces of complexes **Ir-1–Ir-4** are exclusively localized on the styryl BODIPY moieties (Fig. 9), the Ir(III) centres made no contribution suggesting that the triplet states are in the <sup>3</sup>IL state of the respective complexes, which is in full agreement with the nanosecond time-resolved transient absorption of the complexes.<sup>24d,28,50e,52</sup> However, the spin density surface of **Ir-0** is distributed on the ppy ligand as well as on the Ir(III) coordination center. Thus, this result was in agreement with the LLCT/MLCT assignment of **Ir-0**.

The ground state geometries of the complexes were optimized. Slightly distorted conformations were observed for styryl BODIPY moieties (Fig. 10, 11, and S54†). The deviation from the coplanar geometry is more significant for **Ir-4** (Fig. S55†).

The UV-Vis absorption of the complexes was calculated based on the optimized ground state geometry (Franck–Condon principle).<sup>53,54</sup> The calculated UV-Vis absorption band of **Ir-1** is at 643 nm (1.93 eV), which is close to the experimental result at 606 nm (2.05 eV, Fig. 1b). The main transition for this

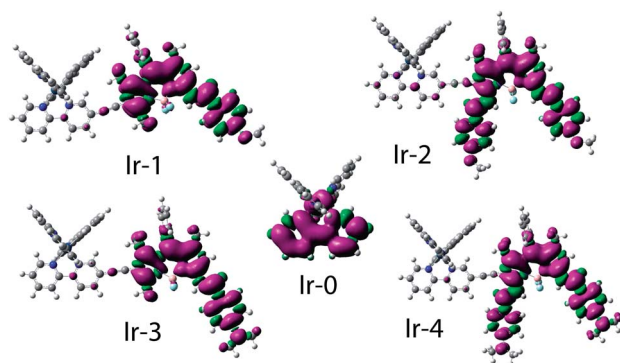


Fig. 9 Isosurfaces of the spin density of the complexes at the optimized triplet state geometry calculated at the B3LYP/LANL2DZ level with Gaussian 09W.

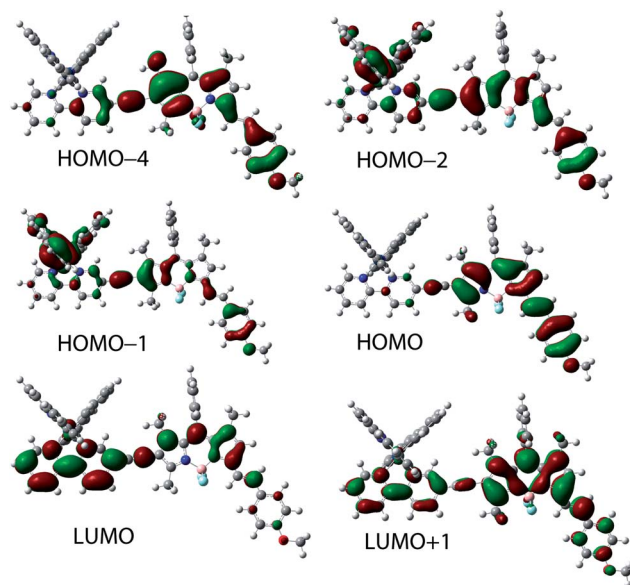


Fig. 10 Electron density maps of the frontier molecular orbital of complex **Ir-1**, based on the ground state optimized geometry by the DFT calculations at the B3LYP/LANL2DZ level with Gaussian 09W.

absorption band is HOMO  $\rightarrow$  LUMO. Based on the molecular orbitals in the low-lying singlet excited states of this transition, it is clear that this transition is styryl BODIPY ligand localized transition (Fig. 10), which is in agreement with the experimental results. The energy gap between the ground state ( $S_0$ ) and the triplet excited states ( $T_1$ ) of **Ir-1** calculated by the TDDFT is predicted as 1.23 eV. The molecular orbitals involved in the transitions of  $T_1$  states are mainly localized styryl BODIPY ligands (Fig. 10 and Table 1). Therefore, the  $T_1$  state can be identified as the <sup>3</sup>IL state, which is in agreement with the spin density analysis and the transient absorption studies.<sup>27a</sup>

Similar calculations were carried out for **Ir-2**. The calculated absorption band is at 738 nm (1.68 eV), which is longer than the experimental results (1.87 eV, 664 nm, Fig. 1b). Molecular orbitals of HOMO  $\rightarrow$  LUMO are involved in this  $S_0 \rightarrow S_1$  transition (Fig. 11 and Table 2). These molecular orbitals are also styryl BODIPY ligand localized, which is in agreement with the UV-Vis absorption spectra (Fig. 1b). The  $S_0 \rightarrow T_1$  energy gap was estimated with the TDDFT method as 1.10 eV. Since the major component of the  $S_0 \rightarrow T_1$  state is HOMO  $\rightarrow$  LUMO+1, the  $T_1$  state can be identified as the <sup>3</sup>IL state since the molecular orbitals are localized on the styryl BODIPY ligand. This result is also in agreement with the spin density analysis and the transient absorption spectroscopy (Fig. 11 and Table 1). For **Ir-3** (see ESI, Fig. S54 and Table S2†) and **Ir-4** (see ESI, Fig. S55 and Table S3†) also, analogous calculations were carried out; the results are similar to those of **Ir-1** and **Ir-2**. The  $S_0 \rightarrow T_1$  energy gaps, calculated with the TDDFT method were found to be 1.14 eV and 1.02 eV for **Ir-3** and **Ir-4**, respectively. For both the complexes **Ir-3** and **Ir-4** <sup>3</sup>IL states were also identified for  $T_1$  states.

The excitations of **Ir-0** were also studied by TDDFT calculations. The calculated UV-Vis absorption band was at 387 nm which is in agreement with the experimental results (385 nm).

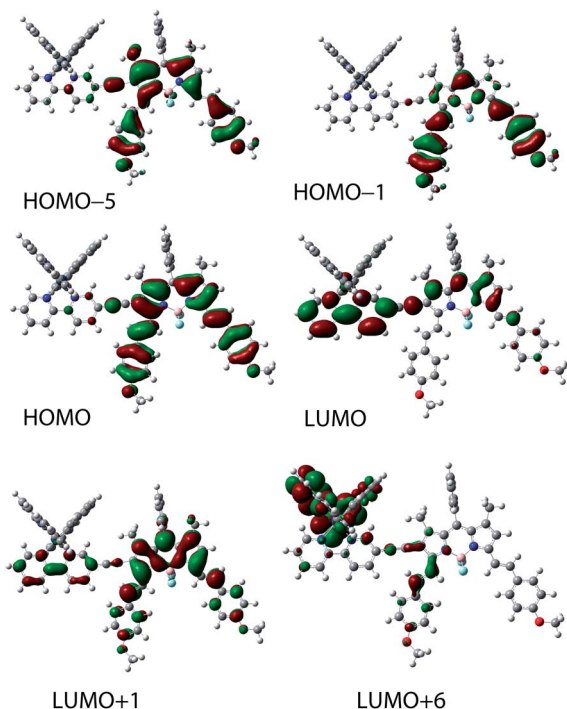


Fig. 11 Electron density maps of the frontier molecular orbitals of complex Ir-2. Based on the ground state optimized geometry by the DFT calculations at the B3LYP/LANL2DZ level with Gaussian 09W.

The Ir(III) atom and ppy ligands contributed to the transitions, could be assigned as MLCT or LLCT transitions (see ESI, Fig. S56 and Table S4†). The  $S_0 \rightarrow T_1$  energy gap was found to be 2.64 eV (470 nm, 2.64 eV), which was in good agreement with the observed RT phosphorescence emission at 507 nm (2.45 eV) indicating that the  $T_1$  state could be assigned as LLCT or MLCT (see ESI, Fig. S56 and Table S4†). These parameters are comparable to the experimental results of the complexes (Table 3).

### Photosensitization of singlet oxygen ( $^1O_2$ ): photooxidation with the complexes as a triplet photosensitizer

As the complexes show strong absorption of visible light and long-lived triplet excited states (Table 3), these are applicable in

photocatalysis as a singlet oxygen ( $^1O_2$ ) photosensitizer. Herein, the  $^1O_2$  photosensitizing ability of the complexes as triplet photosensitizers were studied with visible light photooxidation using DHN as the  $^1O_2$  scavenger to follow the kinetics of the  $^1O_2$  production of the triplet photosensitizers. The photooxidation product juglone thus formed can be used for preparation of anti-cancer compounds.<sup>55</sup> The conventional triplet photosensitizers *meso*-tetraphenylporphyrin (TPP) and methylene blue (MB) were studied for comparison. The consumption of DHN can be monitored by the decrease in its absorption at 301 nm signifying the progress of  $^1O_2$  photosensitizing with Ir(III).<sup>49,56</sup>

The UV-Vis absorption spectra of the mixture were monitored (Fig. 12 and S57†). The more efficient changes were found for Ir-2 than other complexes. However, for Ir-1, the decrease of the DHN absorption at 301 nm occurs at a much lesser extent than that of Ir-2. The absorption of all the complexes in the visible region did not change upon continuous irradiation, therefore the photostability of the complexes is good. Significant changes were found for TPP and MB (Fig. S57b and S57c†).

The photooxidation velocities with Ir(III) complexes as the triplet photosensitizers were compared with MB and TPP by plotting the  $\ln(C_t/C_0)$  against the irradiation time (Fig. 13a). The larger the slope of the plot, the more efficient the  $^1O_2$  photosensitizing ability. Ir-2 is more efficient than MB ( $\Phi_\Delta = 65\%$ ).<sup>57</sup> Ir-3 and Ir-0 show much weaker  $^1O_2$  photosensitizing ability. Ir-0 shows weaker  $^1O_2$  photosensitizing ability due to the lack of visible light-harvesting. Ir-4 is the photosensitizer that gives the poorest performance. The parameters related to photooxidation of DHN using the Ir(III) complexes, MB and TPP are summarized in Table 4. Ir-1 and Ir-2 show  $\Phi_\Delta$  values of 53% and 81%, respectively, thus these complexes are efficient  $^1O_2$  photosensitizers. The absorption of Ir-2 in the visible region is much stronger than that of Ir-1, therefore the  $^1O_2$  photosensitizing ability of Ir-2 is much more efficient than Ir-1. Ir-3 and Ir-4 show a very low yield of 6% and 2%, respectively, which may be responsible for the poor  $^1O_2$  photooxidation ability of Ir-3 and Ir-4. Ir-2 as a photosensitizer on photoirradiation for 40 min, yielded 91% of juglone, which is higher than the other Ir(III) complexes and MB (Fig. 13a and Table 4). Ir-4 yielded only 41% of juglone due to low singlet oxygen quantum yield ( $\Phi_\Delta$ ). It should be pointed out that the photooxidation of the complexes are dependent on the intrinsic properties of the triplet

Table 2 Electronic excitation energies (eV) and corresponding oscillator strengths ( $f$ ), main configurations and CI coefficients of the low-lying electronic excited states of complex Ir-2 calculated by TDDFT//B3LYP/LANL2DZ based on the DFT//B3LYP/LANL2DZ optimized ground state geometries

TDDFT//B3LYP/GENECP						
	Electronic transition	Energy <sup>a</sup> [eV nm <sup>-1</sup> ]	$f^b$	Composition <sup>c</sup>	CI <sup>d</sup>	Character
Singlet	$S_0 \rightarrow S_1$	1.68/738	0.7719	H → L	0.7027	ILCT
	$S_0 \rightarrow S_2$	1.96/633	0.8263	H → L+1	0.7041	ILCT
	$S_0 \rightarrow S_7$	2.68/462	0.6249	H-1 → L+1	0.5402	ILCT
	$S_0 \rightarrow S_{17}$	3.22/385	0.1178	H → L+6	0.6348	LLCT/MLCT
Triplet	$S_0 \rightarrow T_1$	1.10/1130	0.0000 <sup>e</sup>	H → L+1	0.5852	ILCT

<sup>a</sup> Only the selected low-lying excited states are presented. <sup>b</sup> Oscillator strengths. <sup>c</sup> Only the main configurations are presented. <sup>d</sup> The CI coefficients are in absolute values. <sup>e</sup> No spin-orbital coupling effect was considered, thus the  $f$  values are zero.

Table 3 Photophysical properties of ligands and cyclometalated Ir(III) complexes<sup>a</sup>

	$\lambda_{\text{abs}}/\text{nm}$	$\epsilon^b$	$\lambda_{\text{em}}/\text{nm}$	$\Phi_{\text{F}}^c/\%$	$\tau_{\text{F}}^d/\text{ns}$	$\Delta_{\text{st}}^i$	$\tau_{\text{T}}^j$
<b>L1</b>	605/564 <sup>e</sup>	1.030/0.324 <sup>e</sup>	625 <sup>e</sup>	68.6 <sup>e</sup>	4.00 <sup>e</sup>	— <sup>k</sup>	— <sup>k</sup>
	601/556 <sup>f</sup>	1.060/0.345 <sup>f</sup>	624 <sup>f</sup>	6.1 <sup>f</sup>	3.85 <sup>f</sup>	— <sup>k</sup>	— <sup>k</sup>
	593/550 <sup>g</sup>	1.036/0.346 <sup>g</sup>	615 <sup>g</sup>	36.2 <sup>g</sup>	3.70 <sup>g</sup>	— <sup>k</sup>	— <sup>k</sup>
	593/550 <sup>h</sup>	1.029/0.348 <sup>h</sup>	616 <sup>h</sup>	34.4 <sup>h</sup>	3.65 <sup>h</sup>	— <sup>k</sup>	— <sup>k</sup>
<b>L2</b>	666/612 <sup>e</sup>	1.132/0.339 <sup>e</sup>	684 <sup>e</sup>	35.6 <sup>e</sup>	4.48 <sup>e</sup>	— <sup>k</sup>	— <sup>k</sup>
	659/608 <sup>f</sup>	1.039/0.353 <sup>f</sup>	682 <sup>f</sup>	13.5 <sup>f</sup>	4.49 <sup>f</sup>	— <sup>k</sup>	— <sup>k</sup>
	650/601 <sup>g</sup>	1.015/0.355 <sup>g</sup>	676 <sup>g</sup>	12.1 <sup>g</sup>	4.21 <sup>g</sup>	— <sup>k</sup>	— <sup>k</sup>
	650/604 <sup>h</sup>	0.948/0.345 <sup>h</sup>	678 <sup>h</sup>	18.4 <sup>h</sup>	4.76 <sup>h</sup>	— <sup>k</sup>	— <sup>k</sup>
<b>L3</b>	639/590 <sup>e</sup>	1.225/0.466 <sup>e</sup>	674 <sup>e</sup>	24.5 <sup>e</sup>	3.72 <sup>e</sup>	— <sup>k</sup>	— <sup>k</sup>
	636/590 <sup>f</sup>	1.137/0.487 <sup>f</sup>	699 <sup>f</sup>	16.0 <sup>f</sup>	3.52 <sup>f</sup>	— <sup>k</sup>	— <sup>k</sup>
	627 <sup>g</sup>	1.078 <sup>g</sup>	710 <sup>g</sup>	2.1 <sup>g</sup>	0.61 <sup>g</sup>	— <sup>k</sup>	— <sup>k</sup>
	628 <sup>h</sup>	1.035 <sup>h</sup>	714 <sup>h</sup>	1.3 <sup>h</sup>	0.69 <sup>h</sup>	— <sup>k</sup>	— <sup>k</sup>
<b>L4</b>	723 <sup>e</sup>	0.689 <sup>e</sup>	758/679 <sup>e</sup>	10.3 <sup>e</sup>	3.64 ( $\lambda_{\text{em}} = 758$ ) <sup>e</sup>	— <sup>k</sup>	— <sup>k</sup>
					3.10 ( $\lambda_{\text{em}} = 679$ ) <sup>e</sup>		
	720 <sup>f</sup>	0.586 <sup>f</sup>	779/674 <sup>f</sup>	3.4 <sup>f</sup>	2.87 ( $\lambda_{\text{em}} = 779$ ) <sup>f</sup>	— <sup>k</sup>	— <sup>k</sup>
					2.60 ( $\lambda_{\text{em}} = 674$ ) <sup>f</sup>		
<b>Ir-0</b>	709 <sup>g</sup>	0.542 <sup>g</sup>	782 <sup>g</sup>	0.9 <sup>g</sup>	1.14 <sup>g</sup>	— <sup>k</sup>	— <sup>k</sup>
	712 <sup>h</sup>	0.558 <sup>h</sup>	792 <sup>h</sup>	1.0 <sup>h</sup>	1.47 <sup>h</sup>	— <sup>k</sup>	— <sup>k</sup>
	284/385 <sup>e</sup>	0.498/0.151 <sup>e</sup>	507 <sup>e</sup>	— <sup>k</sup>	54.63 <sup>e</sup>	— <sup>k</sup>	1.34 <sup>e</sup>
	282/382 <sup>f</sup>	0.770/0.207 <sup>f</sup>	511 <sup>f</sup>	— <sup>k</sup>	104.74 <sup>f</sup>	— <sup>k</sup>	— <sup>k</sup>
<b>Ir-1</b>	280/378 <sup>g</sup>	0.478/0.133 <sup>g</sup>	513 <sup>g</sup>	— <sup>k</sup>	55.28 <sup>g</sup>	— <sup>k</sup>	— <sup>k</sup>
	280/375 <sup>h</sup>	0.948/0.249 <sup>h</sup>	515 <sup>h</sup>	72.6 <sup>h</sup>	57.08 <sup>h</sup>	— <sup>k</sup>	— <sup>k</sup>
	606/563 <sup>e</sup>	1.138/0.375 <sup>e</sup>	624 <sup>e</sup>	39.9 <sup>e</sup>	2.21 <sup>e</sup>	18 <sup>e</sup>	106.6 <sup>e</sup>
	602/561 <sup>f</sup>	1.176/0.439 <sup>f</sup>	624 <sup>f</sup>	4.7 <sup>f</sup>	0.55 <sup>f</sup>	22 <sup>f</sup>	— <sup>k</sup>
<b>Ir-2</b>	594/554 <sup>g</sup>	1.189/0.434 <sup>g</sup>	615 <sup>g</sup>	6.9 <sup>g</sup>	0.54 <sup>g</sup>	21 <sup>g</sup>	113.2 <sup>g</sup>
	593/552 <sup>h</sup>	1.133/0.420 <sup>h</sup>	616 <sup>h</sup>	11.7 <sup>h</sup>	0.83 <sup>h</sup>	23 <sup>h</sup>	21.0 <sup>h</sup>
	664/610 <sup>e</sup>	0.896/0.346 <sup>e</sup>	691/621 <sup>e</sup>	13.2 <sup>e</sup>	3.86 ( $\lambda_{\text{em}} = 691$ ) <sup>e</sup>	27 <sup>e</sup>	156.5 <sup>e</sup>
					2.47 ( $\lambda_{\text{em}} = 621$ ) <sup>e</sup>		
<b>Ir-3</b>	653/601 <sup>f</sup>	0.982/0.419 <sup>f</sup>	678/613 <sup>f</sup>	6.0 <sup>f</sup>	2.03 ( $\lambda_{\text{em}} = 691$ ) <sup>f</sup>	25 <sup>f</sup>	— <sup>k</sup>
					0.77 ( $\lambda_{\text{em}} = 613$ ) <sup>f</sup>		
	647/596 <sup>g</sup>	0.979/0.411 <sup>g</sup>	673/609 <sup>g</sup>	10.4 <sup>g</sup>	3.04 ( $\lambda_{\text{em}} = 691$ ) <sup>g</sup>	26 <sup>g</sup>	90.8 <sup>g</sup>
					0.96 ( $\lambda_{\text{em}} = 609$ ) <sup>g</sup>		
<b>Ir-4</b>	646/596 <sup>h</sup>	0.896/0.394 <sup>h</sup>	674/611 <sup>h</sup>	13.8 <sup>h</sup>	3.64 ( $\lambda_{\text{em}} = 691$ ) <sup>h</sup>	28 <sup>h</sup>	103.7 <sup>h</sup>
					1.33 ( $\lambda_{\text{em}} = 611$ ) <sup>h</sup>		
	644/596 <sup>e</sup>	0.989/0.438 <sup>e</sup>	683 <sup>e</sup>	32.6 <sup>e</sup>	3.33 <sup>e</sup>	39 <sup>e</sup>	92.5 <sup>e</sup>
	645 <sup>f</sup>	0.949 <sup>f</sup>	716 <sup>f</sup>	1.3 <sup>f</sup>	0.73 <sup>f</sup>	71 <sup>f</sup>	— <sup>k</sup>
<b>Ir-4</b>	633 <sup>g</sup>	0.882 <sup>g</sup>	718 <sup>g</sup>	0.6 <sup>g</sup>	0.35 <sup>g</sup>	85 <sup>g</sup>	37.5 <sup>g</sup>
	632 <sup>h</sup>	0.895 <sup>h</sup>	736 <sup>h</sup>	0.4 <sup>h</sup>	0.45 <sup>h</sup>	104 <sup>h</sup>	61.6 <sup>h</sup>
	729/286 <sup>e</sup>	0.789/1.211 <sup>e</sup>	794/684 <sup>e</sup>	1.0 <sup>e</sup>	2.10 ( $\lambda_{\text{em}} = 794$ ) <sup>e</sup>	65 <sup>e</sup>	31.4 <sup>e</sup>
					2.54 ( $\lambda_{\text{em}} = 684$ ) <sup>e</sup>		
	720 <sup>f</sup>	0.847 <sup>f</sup>	777 <sup>f</sup>	0.2 <sup>f</sup>	0.89 <sup>f</sup>	57 <sup>f</sup>	— <sup>k</sup>
	710 <sup>g</sup>	0.843 <sup>g</sup>	787 <sup>g</sup>	0.23 <sup>g</sup>	0.71 <sup>g</sup>	77 <sup>g</sup>	54.4 <sup>g</sup>
	714 <sup>h</sup>	0.788 <sup>h</sup>	800 <sup>h</sup>	0.18 <sup>h</sup>	0.76 <sup>h</sup>	86 <sup>h</sup>	91.0 <sup>h</sup>

<sup>a</sup>  $c = 1.0 \times 10^{-5}$  M. <sup>b</sup> Molar extinction coefficient at the absorption maxima.  $\epsilon: 10^5 \text{ M}^{-1} \text{ cm}^{-1}$ . <sup>c</sup> Fluorescence quantum yields with complex Ru(dmb)<sub>3</sub>[PF<sub>6</sub>]<sub>2</sub> ( $\Phi_{\text{F}} = 7.3\%$  in MeCN) and BODIPY derivative **7** ( $\Phi_{\text{F}} = 9.3\%$  in toluene) as the standard. <sup>d</sup> Fluorescence lifetimes under an air atmosphere. <sup>e</sup> In toluene. <sup>f</sup> In dichloromethane. <sup>g</sup> In methanol. <sup>h</sup> In acetonitrile. <sup>i</sup> Stokes shift (in nm). <sup>j</sup> Triplet excited state lifetimes, measured by nanosecond time-resolved transient absorptions under the N<sub>2</sub> atmosphere ( $c = 1.0 \times 10^{-5}$  M). <sup>k</sup> Not determined.

photosensitizers (such as the light-harvesting ability and the triplet state lifetimes), but it is also strongly dependent on the match between the absorption spectra of the photosensitizers and the emission spectra of the excitation lamp. The comparison of the absorption spectra of photosensitizers and the emission of excitation lamp was carried out (see ESI, Fig. S57d†). The excitation lamp gives broad emission spectra (not monochromatic light), and there is a good agreement between the absorption spectra of the triplet photosensitizers and the emission spectra. Therefore, the comparison of the photooxidation of the **Ir-1**, **Ir-2**, **Ir-3**, **Ir-4** and the model triplet photosensitizers is reliable: the relative photooxidation ability

of the complexes are directly related to the light-absorbing and the triplet excited state lives of the triplet photosensitizers.

### Fluorescent imaging and intracellular PDT studies

The complexes show fluorescence and intersystem crossing. As a result, the luminescence is independent of oxygen (O<sub>2</sub>), and singlet oxygen (<sup>1</sup>O<sub>2</sub>) can be produced upon photoexcitation. Therefore, these complexes can be used as multi-functional materials. Since, the singlet oxygen quantum yield of **Ir-2** is high, we have explored the cytotoxicity of Ir(III) complexes in LLC cells (lung cancer cells) both in the presence and in the

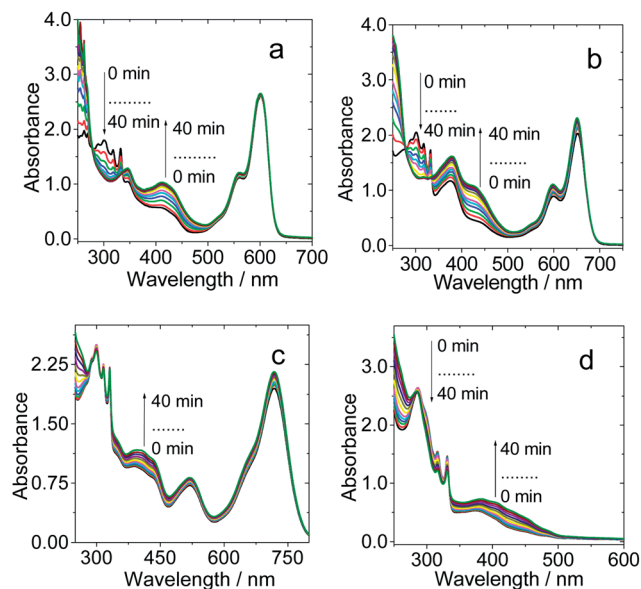


Fig. 12 UV-Vis absorption spectral change for DHN using complex (a) Ir-1, (b) Ir-2, (c) Ir-4, and (d) Ir-0 as photosensitizers. Irradiated with a 35 W xenon lamp ( $20 \text{ mW cm}^{-2}$  in the photoreactor; the UV light with a wavelength shorter than 385 nm was blocked by 0.72 M  $\text{NaNO}_2$  solution). In  $\text{CH}_2\text{Cl}_2$ - $\text{CH}_3\text{OH}$  (9 : 1, v/v); c [DHN] =  $2.0 \times 10^{-4}$  M; c [photosensitizer] =  $2.0 \times 10^{-5}$  M;  $20^\circ\text{C}$ .

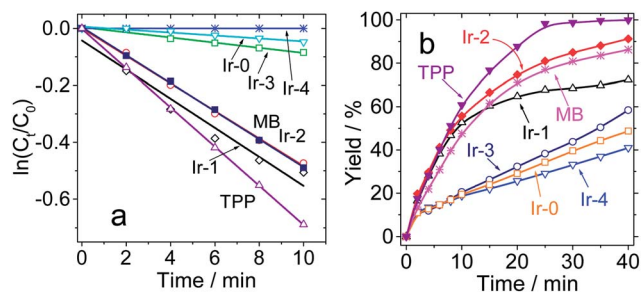


Fig. 13 (a) Plots of  $\ln(C_t/C_0)$  vs. irradiation time ( $t$ ) for the photooxidation of DHN using Ir(III) complexes; (b) plots of chemical yields of juglone vs. irradiation time for the photooxidation of DHN. Irradiated with a 35 W xenon lamp ( $20 \text{ mW cm}^{-2}$  in the photoreactor; the UV light with a wavelength shorter than 385 nm was blocked by 0.72 M  $\text{NaNO}_2$  solution). In  $\text{CH}_2\text{Cl}_2$ - $\text{CH}_3\text{OH}$  (9 : 1, v/v); c [DHN] =  $2.0 \times 10^{-4}$  M; c [photosensitizer] =  $2.0 \times 10^{-5}$  M;  $20^\circ\text{C}$ .

absence of light to investigate the photodynamic therapy (PDT) effect of the complexes. PDT being a non-invasive and attractive protocol in the treatment of a variety of cancer cells by the combined use of near IR or visible light with a photosensitizing drug, has been used to form intracellular reactive oxygen species (ROS) to kill cells and to stimulate the immune response. No IR absorbing Ir(III) complexes have been reported for application in PDT studies.<sup>59,60</sup>

The cells were treated with  $10 \mu\text{M}$  Ir(III) complexes and were kept either in the dark or were illuminated with a 635 nm LED. To ascertain the cellular uptake of the photosensitizers, incubated cells were imaged using a confocal fluorescence microscope (Fig. 14, S58–S60†). Ir-1–Ir-3 exhibits a red fluorescence

Table 4 Pseudo-first-order kinetics parameters,  $^1\text{O}_2$  generation quantum efficiencies and yields of juglone for the photooxidation of DHN using complexes Ir-1, Ir-2, Ir-3, Ir-4, MB and TPP as triplet photosensitizers

	$\tau_T^a$ [ $\mu\text{s}$ ]	$k_{\text{obs}}^b$	$\nu_i^c$	$\Phi_\Delta^d$	Yield <sup>i</sup> [%]
<b>Ir-1</b>	106.6	51.1	1.022	0.53 <sup>e</sup>	72.3
<b>Ir-2</b>	156.5	48.4	0.968	0.81 <sup>f</sup>	91.2
<b>Ir-3</b>	92.5	9.1	0.182	0.06 <sup>g</sup>	58.4
<b>Ir-4</b>	31.4	0	0	0.02 <sup>h</sup>	41.0
<b>Ir-0</b>	1.34	5.2	0.104	—	48.7
<b>MB</b>	83.3	49.1	0.982	0.57	86.2
<b>TPP</b>	82.5	68.9	1.378	0.65	99.9

<sup>a</sup> Triplet excited state lifetimes, measured by nanosecond time-resolved transient absorptions ( $c = 1.0 \times 10^{-5}$  M in toluene). <sup>b</sup> Pseudo-first-order rate constant,  $\ln(C_t/C_0) = -k_{\text{obs}}t$ . In  $10^{-3} \text{ min}^{-1}$ . <sup>c</sup> Initial consumption rate of DHN,  $\nu_i = k_{\text{obs}}[\text{DHN}]$ . In  $10^{-5} \text{ min}^{-1}$ . <sup>d</sup> Singlet oxygen ( $^1\text{O}_2$ ) generation quantum yield measured using methylene blue ( $\Phi_\Delta = 0.57$  in  $\text{CH}_2\text{Cl}_2$ ) as a reference. <sup>e</sup>  $\lambda_{\text{ex}} = 611 \text{ nm}$ . <sup>f</sup>  $\lambda_{\text{ex}} = 652 \text{ nm}$ . <sup>g</sup>  $\lambda_{\text{ex}} = 642 \text{ nm}$ . <sup>h</sup>  $\lambda_{\text{ex}} = 664 \text{ nm}$ . <sup>i</sup> Yield of juglone after photoreaction for 40 min.

signal ( $\lambda_{\text{ex}} = 543 \text{ nm}$ ). The overlay of fluorescence and bright field images, confirm the good cellular permeability of the photosensitizers. In contrast, cellular uptake of Ir-4 was poor in the absence of light. As a control the cells were incubated in the absence of light and also in the absence of sensitizers. No

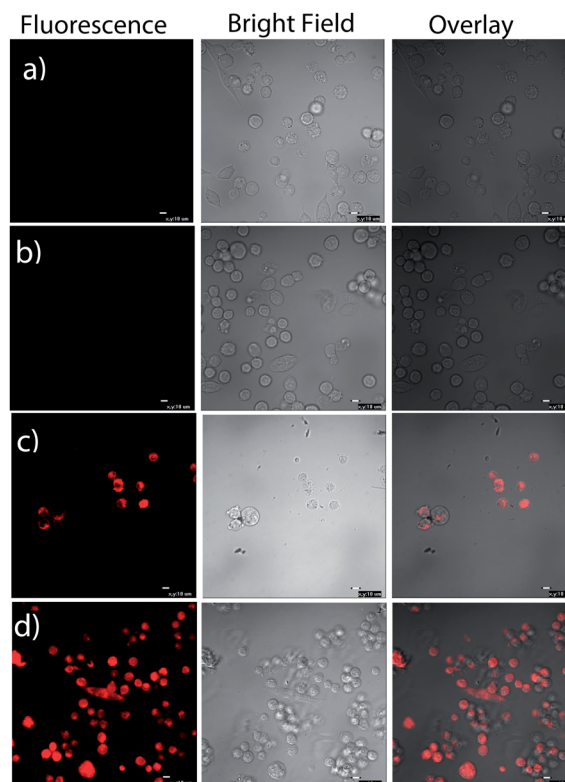


Fig. 14 Confocal fluorescence images in LLC cells. (a) Cells in control on incubation in the dark for 24 h; (b) cells in control on irradiation for 4 hours by a 635 nm LED followed by further incubation in the dark for 24 h; (c) Ir-2 ( $10 \mu\text{M}$ ) treated cells in the dark for 24 h and (d) Ir-2 ( $10 \mu\text{M}$ ) treated cells on irradiation for 4 hours by a 635 nm LED followed by further incubation in the dark for 24 h.

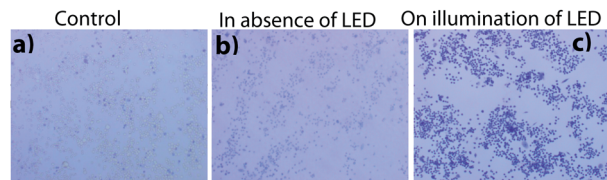


Fig. 15 Trypan blue staining images of LLC cells treated (a) in the absence of LED and photosensitizers, (b) in the absence of LED but in the presence of Ir-2 (10  $\mu\text{M}$ ) and (c) on illumination of LED and Ir-2 (10  $\mu\text{M}$ ).

fluorescence was observed in the respective controls (Fig. 14a and b).

The effect of Ir(III) complexes for cell viability was investigated both in the presence and in the absence of light using trypan blue staining (Fig. 15 and Fig. S61–S64<sup>†</sup>).<sup>58</sup> Trypan blue is one of the dye exclusion procedures for viable cell counting. This method is based on the principle that live (viable) cells do not take up certain dyes, whereas dead (nonviable) cells do. Since cells are very selective to the compound that penetrates through the cell membrane in a viable cell, trypan blue is not absorbed and hence, live cells with undamaged cell membranes are not colored. However, it traverses the membrane of the dead cell and binds to several intracellular proteins, staining the cell blue. Therefore, dead cells are shown to be a distinctive blue color or dark black at the center of the cell as per the background of the image under a light microscope, and living cells are excluded from staining.

Phototoxicity with different concentrations of the Ir-complexes (1  $\mu\text{M}$ , 10  $\mu\text{M}$ , 20  $\mu\text{M}$ ), and different optical doses (1 h, 3 h) was studied. The results show that with increasing the complexes concentration or optical doses, the PDT effect become more significant, especially with increasing the complex concentration (see ESI, Fig. 14, S58, and S59 for detail<sup>†</sup>).

The PDT effect of TPP (tetraphenylporphyrin) under the same condition was studied.<sup>64</sup> The trypan blue staining experiments show that the PDT effect of our Ir-complexes is more significant than TPP (see ESI Fig. S61–S63 and S66 for detail<sup>†</sup>). The reason may be due to the stronger absorption of the Ir-complexes in the visible spectral region as compared with that of TPP. Note that the absorption of porphyrins in the visible spectral region is actually weak (the most intense absorption of porphyrin is at *ca.* 400 nm).

The  $^1\text{O}_2$  production of the complexes in aqueous solution was studied (see ESI Table S1<sup>†</sup>). Aqueous solvent MeOH–H<sub>2</sub>O (4 : 1, v/v) and protic solvent MeOH were used. Ir-1 and Ir-2 show  $\Phi_{\Delta}$  values of 70% and 35%, respectively. However, Ir-3 and Ir-4 show no  $^1\text{O}_2$  production (see ESI Table S1<sup>†</sup>). These results are in agreement with the PDT studies as discussed above. The failure of Ir-3 and Ir-4 to produce  $^1\text{O}_2$  in aqueous solution may be due to the quenching of the triplet states of Ir-3 and Ir-4 by the intramolecular charge transfer (ICT).

IC<sub>50</sub> values of the complexes in the absence of LED illumination were studied (Table 5). 1121 and LLC cell lines were cultured as described in the main manuscript. The IC<sub>50</sub> values

Table 5 IC<sub>50</sub> values of Ir-1 and Ir-2 ( $\mu\text{M}$ )<sup>a</sup>

Cell	Ir-1		Ir-2	
	In dark	On photoirradiation	In dark	On photoirradiation
1121	9.81	2.58	16.70	7.68
LLC	8.16	6.18	15.63	9.80

<sup>a</sup> IC<sub>50</sub>, the concentration of compound that inhibits the proliferation rate by 50% compared with control untreated cells. Irradiated by a 635 nm LED.

of Ir-1 and Ir-2 for different concentrations of 0, 1, 2, 4, 8, 16, and 25  $\mu\text{M}$  in cells were investigated both in the absence and in the presence of light for 36 h using the MTT assay.<sup>62</sup> Cells were incubated with different concentrations 0, 1, 2, 4, 8, 16, and 25  $\mu\text{M}$  of Ir-1 and Ir-2 for 36 h. IC<sub>50</sub> values for Ir-1 on photoirradiation and in the dark were found to be 2.58 and 9.81  $\mu\text{M}$ , respectively for 1121 cell lines. For LLC cell lines the respective values were 6.18 and 8.16  $\mu\text{M}$ . Similarly, IC<sub>50</sub> values for Ir-2 on photoirradiation and in the absence of photoirradiation were found to be 7.68 and 16.70  $\mu\text{M}$ , respectively for 1121 cell lines and for LLC cell lines the values were 9.80 and 15.63  $\mu\text{M}$ , respectively.

## Conclusions

In conclusion, we prepared four styryl-BODIPY-containing heteroleptic C<sup>N</sup> Ir(III) complexes which show strong NIR absorption (644–729 nm), strong NIR fluorescence (700–800 nm), and long-lived triplet excited states (92.5–156.5  $\mu\text{s}$ ). In these complexes the  $\pi$ -conjugation framework of the ligands were connected to the Ir(III) coordination center *via* the C $\equiv$ C bond, with the aim to induce efficient ISC. The photophysical properties of the complexes and the NIR light-harvesting ligands were studied with the steady state and time-resolved absorption/emission spectroscopy, as well as DFT calculations. We found that the complexes are strongly fluorescent, although the  $\pi$ -conjugation is present between the BODIPY ligands and the Ir(III) coordination center. Moderate intersystem crossing (ISC) was observed for the complexes, proved by the population of the long-lived intraligand triplet excited state ( $^3\text{IL}$ ) and the  $^1\text{O}_2$  photosensitizing property. Based on the property of NIR absorption/fluorescence and the reasonable  $^1\text{O}_2$  quantum yield, the complexes were used as multi-functional materials as luminescent bioimaging reagents and in intracellular photodynamic studies. Our results are useful for preparation of NIR-absorbing cyclometalated Ir(III) complexes, and the relevant application of these complexes as multi-functional materials such as a luminescent bioimaging reagent, in PDT and photocatalysis, *etc.*

## Acknowledgements

We thank the NSFC (21073028, 21273028 and 51202207), the Royal Society (UK) and NSFC (China-UK Cost-Share Science Networks, 21011130154), Ministry of Education

(SRFDP-20120041130005) and the Fundamental Research Funds for the Central Universities (DUT14ZD226) for financial support.

## Notes and references

- (a) Q. Zhao, C. Huanga and F. Li, *Chem. Soc. Rev.*, 2011, **40**, 2508–2524; (b) M. Nurunnabi, Z. Khatun, G. R. Reeck, D. Y. Lee and Y.-K. Lee, *Chem. Commun.*, 2013, **49**, 5079–5081.
- (a) T. Myochin, K. Kiyose, K. Hanaoka, H. Kojima, T. Terai and T. Nagano, *J. Am. Chem. Soc.*, 2011, **133**, 3401–3409; (b) F. Yu, P. Li, G. Li, G. Zhao, T. Chu and K. Han, *J. Am. Chem. Soc.*, 2011, **133**, 11030–11033.
- (a) Y. Chi and P.-T. Chou, *Chem. Soc. Rev.*, 2010, **39**, 638–655; (b) P.-T. Chou and Y. Chi, *Chem.–Eur. J.*, 2007, **13**, 380–395; (c) P.-T. Chou, Y. Chi, M.-W. Chung and C.-C. Lin, *Coord. Chem. Rev.*, 2011, **255**, 2653–2665; (d) H. Xiang, J. Cheng, X. Ma, X. Zhou and J. J. Chruma, *Chem. Soc. Rev.*, 2013, **42**, 6128–6185.
- Y. You and W. Nam, *Chem. Soc. Rev.*, 2012, **41**, 7061–7084.
- T. Peng, Y. Yang, Y. Liu, D. Ma, Z. Hou and Y. Wang, *Chem. Commun.*, 2011, **47**, 3150–3152.
- E. Baranoff, E. Orselli, L. Allouche, D. D. Censo, R. Scopelliti, M. Gratzel and M. K. Nazeeruddin, *Chem. Commun.*, 2011, **47**, 2799–2801.
- (a) C.-C. Ko and V. W.-W. Yam, *J. Mater. Chem.*, 2010, **20**, 2063–2070; (b) Y. Tanaka, K. M.-C. Wong and V. W.-W. Yam, *Chem. Sci.*, 2012, **3**, 1185–1191.
- J. Kuwabara, T. Namekawa, M. Haga and T. Kanbara, *Dalton Trans.*, 2012, **41**, 44–46.
- L. He, J. Qiao, L. Duan, G. Dong, D. Zhang, L. Wang and Y. Qiu, *Adv. Funct. Mater.*, 2009, **19**, 2950–2960.
- Y. H. Song, Y. C. Chiu, Y. Chi, Y. M. Cheng, C. H. Lai, P.-T. Chou, K. T. Wong, M. H. Tsai and C. C. Wu, *Chem.–Eur. J.*, 2008, **14**, 5423–5434.
- (a) E. Orselli, R. Q. Albuquerque, P. M. Fransen, R. Frohlich, H. M. Janssen and L. d. Cola, *J. Mater. Chem.*, 2008, **18**, 4579–4590; (b) D. N. Kozhevnikov, V. N. Kozhevnikov, M. Z. Shafikov, A. M. Prokhorov, D. W. Bruce and J. A. G. Williams, *Inorg. Chem.*, 2011, **50**, 3804–3815.
- B. S. Du, C. H. Lin, Y. Chi, J. Y. Hung, M. W. Chung, T. Y. Lin, G. H. Lee, K. T. Wong, P.-T. Chou, W. Y. Hung and H. C. Chiu, *Inorg. Chem.*, 2010, **49**, 8713–8723.
- S. M. Borisov and I. Klimant, *Anal. Chem.*, 2007, **79**, 7501–7509.
- K. K.-W. Lo, B. T.-N. Chan, H.-W. Liu, K. Y. Zhang, S. P.-Y. Li and T. S.-M. Tang, *Chem. Commun.*, 2013, **49**, 4271–4273.
- (a) V. Fernandez-Moreira, F. L. Thorp-Greenwood and M. P. Coogan, *Chem. Commun.*, 2010, **46**, 186–202; (b) Y. Zhou and J. Yoon, *Chem. Soc. Rev.*, 2012, **41**, 52–67.
- Y. Zhou, J. Jia, W. Li, H. Feia and M. Zhou, *Chem. Commun.*, 2013, **49**, 3230–3232.
- Z. Xie, L. Ma, K. E. DeKrafft, A. Jin and W. Lin, *J. Am. Chem. Soc.*, 2010, **132**, 922–923.
- N. Tian, D. Lenkeit, S. Pelz, L. H. Fischer, D. Escudero, R. Schiewek, D. Klink, O. J. Schmitz, L. Gonzalez, M. Schaferling and E. Holder, *Eur. J. Inorg. Chem.*, 2010, 4875–4885.
- K. Koren, S. M. Borisov, R. Saf and I. Klimant, *Eur. J. Inorg. Chem.*, 2011, 1531–1534.
- Q. Zhao, F. Li and C. Huang, *Chem. Soc. Rev.*, 2010, **39**, 3007–3030.
- (a) H. Zeng, F. Yu, J. Dai, H. Sun, Z. Lu, M. Li, Q. Jiang and Y. Huang, *Dalton Trans.*, 2012, **41**, 4878; (b) Y. Li, Y. Liu and M. Zhou, *Dalton Trans.*, 2012, **41**, 3807; (c) L. Murphy, A. Congreve, L. O. Palsson and J. A. G. Williams, *Chem. Commun.*, 2010, **46**, 8743–8745.
- S. Zanarini, M. Felici, G. Valenti, M. Marcaccio, L. Prodi, S. Bonacchi, P. Contreras-Carballada, R. M. Williams, M. C. Feiters, R. J. M. Nolte, L. D. Cola and F. Paolucci, *Chem.–Eur. J.*, 2011, **17**, 4640–4647.
- (a) J. I. Goldsmith, W. R. Hudson, M. S. Lowry, T. H. Anderson and S. Bernhard, *J. Am. Chem. Soc.*, 2005, **127**, 7502–7510; (b) Sk. Jasimuddin, T. Yamada, K. Fukujū, J. Otsuki and K. Sakai, *Chem. Commun.*, 2010, **46**, 8466–8468; (c) S. Takizawa, R. Aboshi and S. Murata, *Photochem. Photobiol. Sci.*, 2011, **10**, 895–903; (d) S.-y. Takizawa, C. Perez-Bolivar, P. Anzenbacher Jr and S. Murata, *Eur. J. Inorg. Chem.*, 2012, 3975–3979; (e) J. Zhao, W. Wu, J. Sun and S. Guo, *Chem. Soc. Rev.*, 2013, **42**, 5323–5351; (f) J. Sun, F. Zhong and J. Zhao, *Dalton Trans.*, 2013, **42**, 9595–9605.
- (a) W. Zhao and F. N. Castellano, *J. Phys. Chem. A*, 2006, **110**, 11440–11445; (b) T. N. Singh-Rachford and F. N. Castellano, *Coord. Chem. Rev.*, 2010, **254**, 2560–2573; (c) J. Zhao, S. Ji and H. Guo, *RSC Adv.*, 2011, **1**, 937–950; (d) J. Sun, W. Wu, H. Guo and J. Zhao, *Eur. J. Inorg. Chem.*, 2011, 3165–3173.
- (a) F. Gärtner, S. Denurra, S. Losse, A. Neubauer, A. Boddien, A. Gopinathan, A. Spannenberg, H. Junge, S. Lochbrunner, M. Blug, S. Hoch, J. Busse, S. Gladiali and M. Beller, *Chem.–Eur. J.*, 2012, **18**, 3220–3225; (b) B. F. DiSalle and S. Bernhard, *J. Am. Chem. Soc.*, 2011, **133**, 11819–11821; (c) F. Gärtner, D. Cozzula, S. Losse, A. Boddien, G. Anilkumar, H. Junge, T. Schulz, N. Marquet, A. Spannenberg, S. Gladiali and M. Beller, *Chem.–Eur. J.*, 2011, **17**, 6998–7006.
- X. Wang, J. Jia, Z. Huang, M. Zhou and H. Fei, *Chem.–Eur. J.*, 2011, **17**, 8028–8032.
- (a) J. Zhao, S. Ji, W. Wu, W. Wu, H. Guo, J. Sun, H. Sun, Y. Liu, Q. Li and L. Huang, *RSC Adv.*, 2012, **2**, 1712–1728; (b) C. E. McCusker, D. Hablot, R. Ziessel and F. N. Castellano, *Inorg. Chem.*, 2012, **51**, 7957–7959.
- (a) W. Wu, J. Zhao, H. Guo, J. Sun, S. Ji and Z. Wang, *Chem.–Eur. J.*, 2012, **18**, 1961–1968; (b) J. Sun, F. Zhong, X. Yi and J. Zhao, *Inorg. Chem.*, 2013, **52**, 6299–6310.
- (a) O. Buyukcakir, O. A. Bozdemir, S. Kolemen, S. Erbas and E. U. Akkaya, *Org. Lett.*, 2009, **11**, 4644–4647; (b) J.-S. Lu, H. Fu, Y. Zhang, Z. J. Jakubek, Y. Tao and S. Wang, *Angew. Chem., Int. Ed.*, 2011, **50**, 11658–11662; (c) T. Bura, D. Hablot and R. Ziessel, *Tetrahedron Lett.*, 2011, **52**, 2370–2374.
- M. Lepeltier, T. K.-M. Lee, K. K.-W. Lo, L. Toupet, H. L. Bozec and V. Guerschais, *Eur. J. Inorg. Chem.*, 2007, 2734–2747.
- (a) H.-s. Lee and Y. Ha, *Mol. Cryst. Liq. Cryst.*, 2010, **520**, 60/[336]–67/[343]; (b) J. C. Araya, J. Gajardo, S. A. Moya,

- P. Aguirre, L. Toupet, J. A. G. Williams, M. Escadeillas, H. L. Bozec and V. Guerschais, *New J. Chem.*, 2010, **34**, 21–24.
- 32 F. Nastasi, F. Puntoriero, S. Campagna, J.-H. Olivier and R. Ziessel, *Phys. Chem. Chem. Phys.*, 2010, **12**, 7392–7402.
- 33 E. K. Pefkianakis, N. P. Tzanetos and J. K. Kallitsis, *Chem. Mater.*, 2008, **20**, 6254–6262.
- 34 M. S. Lowry, W. R. Hudson, R. A. Pascal and S. Bernhard, *J. Am. Chem. Soc.*, 2004, **126**, 14129–14135.
- 35 J. Sun, W. Wu and J. Zhao, *Chem.–Eur. J.*, 2012, **18**, 8100–8112.
- 36 W. Wu, H. Guo, W. Wu, S. Ji and J. Zhao, *J. Org. Chem.*, 2011, **76**, 7056–7064.
- 37 M. J. Frisch, *et al.*, *Gaussian 09, Revision 01*, Gaussian Inc., Wallingford, CT, 2009.
- 38 Y. Cakmak, S. Kolemen, S. Duman, Y. Dede, Y. Dolen, B. Kilic, Z. Kostereli, L. T. Yildirim, A. L. Dogan, D. Guc and E. U. Akkaya, *Angew. Chem., Int. Ed.*, 2011, **50**, 11937–11941.
- 39 F. Wilkinson, W. P. Helman and A. B. Ross, *J. Phys. Chem. Ref. Data*, 1993, **22**, 113–150.
- 40 A. A. Rachford, S. Goeb and F. N. Castellano, *J. Am. Chem. Soc.*, 2008, **130**, 2766–2767.
- 41 (a) L. Liu, D. Huang, S. M. Draper, X. Yi, W. Wu and J. Zhao, *Dalton Trans.*, 2013, **42**, 10694–10706; (b) L. Ma, S. Guo, J. Sun, C. Zhang, J. Zhao and H. Guo, *Dalton Trans.*, 2013, **42**, 6478–6488; (c) X. Yi, J. Zhao, J. Sun, S. Guo and H. Zhang, *Dalton Trans.*, 2013, **42**, 2062–2074; (d) W. Wu, J. Zhao, J. Sun, L. Huang and X. Yi, *J. Mater. Chem. C*, 2013, **1**, 705–716; (e) W. Wu, D. Huang, X. Yi and J. Zhao, *Dyes Pigm.*, 2013, **96**, 220–231; (f) L. Ma, H. Guo, Q. Li, S. Guo and J. Zhao, *Dalton Trans.*, 2012, **41**, 10680–10689; (g) H. Sun, H. Guo, W. Wu, X. Liu and J. Zhao, *Dalton Trans.*, 2011, **40**, 7834–7841; (h) W. Wu, W. Wu, S. Ji, H. Guo and J. Zhao, *Dalton Trans.*, 2011, **40**, 5953–5963; (i) W. Wu, J. Sun, S. Ji, W. Wu, J. Zhao and H. Guo, *Dalton Trans.*, 2011, **40**, 11550–11561.
- 42 S. Niu, G. Ulrich, P. Retailleau and R. Ziessel, *Org. Lett.*, 2011, **13**, 4996–4999.
- 43 R. Ziessel, T. Bura and J.-H. Olivier, *Synlett*, 2010, 2304.
- 44 S. Zhu, J. Zhang, G. K. Vegesna, R. Pandey, F.-T. Luo, S. A. Green and H. Liu, *Chem. Commun.*, 2011, **47**, 3508–3510.
- 45 Y. H. Yu, A. Descalzo, Z. Shen, H. Rohr, Q. Liu, Y. W. Wang, M. Spieles, Y. Z. Li, K. Rurack and X. Z. You, *Chem. – Asian J.*, 2006, **1**, 176–187.
- 46 S. Kolemen, O. A. Bozdemir, Y. Cakmak, G. Barin, S. Erten-Ela, M. Marszalek, J.-H. Yum, S. M. Zakeeruddin, M. K. Nazeeruddin, M. Gratzel and E. U. Akkaya, *Chem. Sci.*, 2011, **2**, 949–954.
- 47 (a) A. J. Hallett, B. M. Kariuki and S. J. A. Pope, *Dalton Trans.*, 2011, **40**, 9474–9481; (b) A. M. Talarico, E. I. Szerb, T. F. Mastropietro, I. Aiello, A. Crispinia and M. Ghedini, *Dalton Trans.*, 2012, **41**, 4919–4926; (c) L. Flamigni, A. Barbieri, C. Sabatini, B. Ventura and F. Barigelletti, *Top. Curr. Chem.*, 2007, **281**, 143–203; (d) J. A. G. Williams, *Top. Curr. Chem.*, 2007, **281**, 205–268; (e) D. C. Goldstein, Y. Y. Cheng, T. W. Schmidt, M. Bhadbhade and P. Thordarson, *Dalton Trans.*, 2011, **40**, 2053–2061; (f) C.-H. Lin, C.-Y. Lin, J.-Y. Hung, Y.-Y. Chang, Y. Chi, M.-W. Chung, Y.-C. Chang, C. Liu, H.-A. Pan, G.-H. Lee and P.-T. Chou, *Inorg. Chem.*, 2012, **51**, 1785–1795.
- 48 A. A. Rachford, R. Ziessel, T. Bura, P. Retailleau and F. N. Castellano, *Inorg. Chem.*, 2010, **49**, 3730–3736.
- 49 L. Huang, X. Yu, W. Wu and J. Zhao, *Org. Lett.*, 2012, **14**, 2594–2597.
- 50 (a) C. L. Ho, Q. Wang, C. S. Lam, W. Y. Wong, D. Ma, L. Wang, Z. Q. Gao, C. H. Chen, K. W. Cheah and Z. Lin, *Chem. – Asian J.*, 2009, **4**, 89–103; (b) S. Develay, O. Blackburn, A. L. Thompson and J. A. G. Williams, *Inorg. Chem.*, 2008, **47**, 11129–11142; (c) M. D. Perez, P. I. Djurovich, A. Hassan, G. Y. Cheng, T. J. Stewart, K. Aznavour, R. Bau and M. E. Thompson, *Chem. Commun.*, 2009, 4215–4217; (d) Y. Liu, K. Ye, Y. Fan, W. Song, Y. Wang and Z. Hou, *Chem. Commun.*, 2009, 3699–3701; (e) L. Huang, L. Zeng, H. Guo, W. Wu, W. Wu, S. Ji and J. Zhao, *Eur. J. Inorg. Chem.*, 2011, 4527–4533; (f) B. L. Guennic, O. Maurya and D. Jacquemin, *Phys. Chem. Chem. Phys.*, 2012, **14**, 157–164; (g) J.-L. Jin, H.-B. Li, Y. Geng, Y. Wu, Y.-A. Duan and Z.-M. Su, *ChemPhysChem*, 2012, **13**, 3714–3722.
- 51 K. Hanson, A. Tamayo, V. V. Diev, M. T. Whited, P. I. Djurovich and M. E. Thompson, *Inorg. Chem.*, 2010, **49**, 6077–6084.
- 52 Y. Liu and J. Zhao, *Chem. Commun.*, 2012, **48**, 3751–3753.
- 53 B. Valeur, *Molecular Fluorescence: Principles and Applications*, Wiley-VCH Verlag, GmbH, 2001.
- 54 N. J. Turro, V. Ramamurthy and J. C. Scaiano, *Principles of Molecular Photochemistry: An Introduction*, University Science Books, Sausalito, CA, 2009.
- 55 J. Benites, J. A. Valderrama, K. Bettega, R. C. Pedrosa, P. B. Calderon and J. Verrax, *Eur. J. Med. Chem.*, 2010, **45**, 6052–6057.
- 56 (a) J. Sun, J. Zhao, H. Guo and W. Wu, *Chem. Commun.*, 2012, **48**, 4169–4171; (b) N. Adarsh, M. Shanmugasundaram, R. R. Avirah and D. Ramaiah, *Chem.–Eur. J.*, 2012, **18**, 12655–12662.
- 57 M. Korinek, R. Dedic, A. Svoboda and J. Hala, *J. Fluoresc.*, 2004, **14**, 71–74.
- 58 (a) H. Jeong, M. Huh, S. J. Lee, H. Koo, I. C. Kwon, S. Y. Jeong and K. Kim, *Theranostics*, 2011, **1**, 230–239; (b) M. E. Katsarou, E. K. Efthimiadou, G. Psomas, A. Karaliota and D. Vourloumis, *J. Med. Chem.*, 2008, **51**, 470–478; (c) H. Thomadaki, A. Karaliota, C. Litos and A. Scorilas, *J. Med. Chem.*, 2008, **51**, 3713–3719; (d) V. Vergaro, E. Abdullayev, Y. M. Lvov, A. Zeitoun, R. Cingolani, R. Rinaldi and S. Leporatti, *Biomacromolecules*, 2010, **11**, 820–826; (e) H. Thomadaki, A. Karaliota, C. Litos and A. Scorilas, *J. Med. Chem.*, 2007, **50**, 1316–1321.
- 59 (a) A. Gorman, J. Killoran, C. O'Shea, T. Kenna, W. M. Gallagher and D. F. O'Shea, *J. Am. Chem. Soc.*, 2004, **126**, 10619–10631; (b) G. Liang, L. Wang, Z. Yang, H. Koon, N. Mak, C. K. Chang and B. Xu, *Chem. Commun.*, 2006, 5021–5023; (c) T. J. Dougherty, C. J. Gomer, B. W. Henderson, G. Jori, D. Kessel, M. Korbelik, J. Moan and Q. Peng, *J. Natl. Cancer Inst.*, 1998, **90**, 889–905; (d)

- D. Kessel, T. J. Dougherty and C. K. Chang, *Photochem. Photobiol.*, 1991, **53**, 475–479; (e) D. Kessel, Y. Luo, Y. Q. Deng and C. K. Chang, *Photochem. Photobiol.*, 1997, **65**, 422–426; (f) M. R. Detty, S. L. Gibson and S. J. Wagner, *J. Med. Chem.*, 2004, **47**, 3897–3915; (g) S. Banfi, E. Caruso, S. Caprioli, L. Mazzagatti, G. Canti, R. Ravizza, M. Gariboldi and E. Monti, *Bioorg. Med. Chem.*, 2004, **12**, 4853–4860.
- 60 (a) M. Gonzalez-Alvarez, A. Pascual-Alvarez, L. d. C. Agudo, A. Castiñeiras, M. Liu-Gonzalez, J. Borrás and G. Alzuet-Pina, *Dalton Trans.*, 2013, **42**, 10244–10259; (b) S. H. Lim, C. Thivierge, P. Nowak-Sliwinska, J. Han, H. v. d. Bergh, G. Wagnieres, K. Burgess and H. B. Lee, *J. Med. Chem.*, 2010, **53**, 2865–2874; (c) Y. Yang, Q. Guo, H. Chen, Z. Zhou, Z. Guo and Z. Shen, *Chem. Commun.*, 2013, **49**, 3940–3942; (d) Y. Cakmak, S. Kolemen, S. Duman, Y. Dede, Y. Dolen, B. Kilic, Z. Kostereli, L. T. Yildirim, A. L. Dogan, D. Guc and E. U. Akkaya, *Angew. Chem., Int. Ed.*, 2011, **50**, 11937–11941; (e) T. Guo, L. Cui, J. Shen, R. Wang, W. Zhu, Y. Xu and X. Qian, *Chem. Commun.*, 2013, **49**, 1862–1864; (f) E. B. Veale, D. O. Frimannsson, M. Lawler and T. Gunnlaugsson, *Org. Lett.*, 2009, **11**, 4040–4043.
- 61 A. P. Thomas, P. S. S. Babu, S. A. Nair, S. Ramakrishnan, D. Ramaiah, T. K. Chandrashekar, A. Srinivasan and M. R. Pillai, *J. Med. Chem.*, 2012, **55**, 5110–5120.
- 62 (a) J. F. Lovell, M. W. Chan, Q. Qi, J. Chen and G. Zheng, *J. Am. Chem. Soc.*, 2011, **133**, 18580–18582; (b) R. B. P. Elmes, M. Erby, S. M. Cloonan, S. J. Quinn, D. C. Williams and T. Gunnlaugsson, *Chem. Commun.*, 2011, **47**, 686–688.